

Advanced Multi-Product Coal Utilization By-Product Processing Plant

Technical Progress Report for the Period July 31, 2003 to December 31, 2004

Principal Authors: Robert Jewell, Thomas Robl and John Groppo

March 2005

U. S. Department of Energy Cooperative Agreement No. DE-FC26-03NT410781

Center for Applied Energy Research
2540 Research Park Drive
University of Kentucky
Lexington, KY 40511

DISCLAIMER

This report was prepared as an account of work sponsored by an agency of the United States Government. Neither the United States Government nor any agency thereof, nor any employees, makes any warranty, expressed or implied, or assumes any legal liability or responsibility for the accuracy, completeness, or usefulness of any information, apparatus, product, or process disclosed, or represents that its use would not infringe privately owned rights. Reference herein to any specific commercial product, process, or service by trade name, trademark, manufacturer, or otherwise does not necessarily constitute or imply its endorsement, recommendation, or favoring by the United States Government or any agency thereof. The views and opinions of the authors expressed herein do not necessarily state or reflect that of those of the United States Government or any agency thereof.

ABSTRACT

The objective of the project is to build a multi-product ash beneficiation plant at Kentucky Utilities 2,200-MW Ghent Generating Station, located in Carroll County, Kentucky. This part of the study includes the examination of the feedstocks for the beneficiation plant. The ash, as produced by the plant, and that stored in the lower pond were examined.

The ash produced by the plant was found to be highly variable as the plant consumes high and low sulfur bituminous coal, in Units 1 and 2 and a mixture of sub-bituminous and bituminous coal in Units 3 and 4. The ash produced reflected this consisting of an iron-rich (~24%, Fe_2O_3), aluminum rich (~29% Al_2O_3) and high calcium (6% - 7%, CaO) ash, respectively. The LOI of the ash typically was in the range of 5.5% to 6.5%, but individual samples ranged from 1% to almost 9%.

The lower pond at Ghent is a substantial body, covering more than 100 acres, with a volume that exceeds 200 million cubic feet. The sedimentation, stratigraphy and resource assessment of the in place ash was investigated with vibracoring and three-dimensional, computer-modeling techniques. Thirteen cores to depths reaching nearly 40 feet, were retrieved, logged in the field and transported to the lab for a series of analyses for particle size, loss on ignition, petrography, x-ray diffraction, and x-ray fluorescence.

Collected data were processed using ArcViewGIS, Rockware, and Microsoft Excel to create three-dimensional, layered iso-grade maps, as well as stratigraphic columns and profiles, and reserve estimations. The ash in the pond was projected to exceed 7 million tons and contain over 1.5 million tons of coarse carbon, and 1.8 million tons of fine (<10 μm) glassy pozzolanic material. The size, quality and consistency of the ponded material suggests that it is the better feedstock for the beneficiation plant.

TABLE OF CONTENTS

Section	Page No.
Disclaimer.....	2
Abstract.....	3
List of Graphical Materials.....	5
Executive Summary.....	7
Introduction.....	9
Experimental.....	10
Ash and Coal Collection and Characterization from the Ghent Power Plant.....	10
The Coring and Analysis of Ash in the Lower Pond at Ghent.....	10
Pond Core Analysis.....	13
Sediment Types.....	13
Results and Discussion.....	18
The Characterization and Assessment of the Lower Ash Pond.....	23
Introduction.....	23
The Coring of the Lower Pond.....	23
Dry-Sieve Analysis.....	25
Particle-Size Analyses.....	25
Loss-On-Ignition Analyses.....	25
Mineralogical and Chemical Analysis.....	32
Pond Mapping.....	38
Iso-Grade Analysis.....	39
Reserve Estimations.....	41
Conclusions.....	42
Reference.....	43
Appendices	
Appendix A: Sedimentologic Columns.....	44
Appendix B: Vibracore Analysis Data.....	57

LIST OF GRAPHICAL MATERIALS

Figure 1	Photo of Argo with vibracore apparatus.....	10
Figure 2	Sedimentologic column of vibracore-hole 16.....	16
Figure 3	Dry-sieve analysis results of cored samles.....	25
Figure 4	Chart illustrating the distribution of average weight percent for the >100 fraction of ash.....	26
Figure 5	Mean particle-size data by hole.....	26
Figure 6	Chart illustrating average particle-size distribution of the <100 fraction of ash, in 5-foot intervals.....	28
Figure 7	Scatter plot of the mean particle size for the <100 fraction of samples analyzed.....	28
Figure 8	Loss-on-ignition data for each of the cored holes, plotted as a function of mean particle size for the <100 fraction.....	29
Figure 9a	Loss-on-ignition data displayed as a function of weight for the silt to fine sand-size fraction.....	29
Figure 9b	Loss-on-ignition data displayed as a function of weight for the medium-sand to coarse-gravel fraction.....	29
Figure 10	Average percentages of unburned carbon for the <100-mesh and >100-mesh size-fractions.....	30
Figure 11	Diffractiongram of a brown ash from hole 15, at a depth of 26.3 to 28 feet (8 to 8.5 m).....	33
Figure 12	Diffractiongram of a tan ash from hole 16, at a depth of 28.1 to 29.7 feet (8.6 to 9.1 m).....	33
Figure 13	Diffractiongram of a light-gray ash from hole 10, at a depth of 25.2 to 26.5 feet (7.7 to 8.1m).....	34
Figure 14	Diffractiongram of a dark-gray ash from hole 18, at a depth of 19.1 to 21.2 feet (5.8 to 6.5 m).....	34
Figure 15	Petrographic image of glassy fly-ash particles.....	35
Figure 16	Petrographic image of a sand-size carbon particle surrounded by <10 μ m, glassy, fly-ash spheres.....	35
Figure 17	Microscopic image of a coarsening-upward fly-ash interval.....	36
Figure 18	Microscopic image of cyclic laminae and small-scale sedimentary structures.....	36
Figure 19	Vibracore-hole location map.....	37
Figure 20	Example of map created using statistical contouring methods.....	37
Figure 21	Stacked iso-grade maps for the average percent of unburned coarse carbon.....	38

Table 1	An example of the data collected from each vibracore hole.....	11
Table 2	Ultimate analysis of a coal used at Ghent Power Plant.....	17
Table 3	Major element analysis of coal ash.....	17
Table 4	Trace element analysis of coal ash in ppm.....	17
Table 5	Ultimate, ash and LOI analysis of Ghent fly ash by ESP field.....	18
Table 6	Major element oxide data for fly ash samples by unit and ESP field.....	19
Table 7	Trace element data for fly ash.....	20
Table 8	Bottom ash analysis for Ghent units.....	21
Table 9	Vibracore-hole depth data.....	23
Table 10	Dry-sieve analysis results using a No.100-mesh sieve.....	25
Table 11	Data used to compile the bar chart in Figure 4.....	27
Table 12	Typical chemistry of coal fly ash (in weight percent).....	32
Table 13	XRF data from the analyses, on core samples, that represent the four typical colors of fly ash.....	32
Table 14	>100-mesh, LOI data used to compile the iso-grade maps in Figure 21.....	39
Table 15	Reserve estimates for the drilled area of the pond.....	40
Table 16	Reserve estimates for the entire pond.....	40

EXECUTIVE SUMMARY

The project area is located in Carroll County, Kentucky, approximately one mile northeast of Ghent, Kentucky. The lower ash pond is situated immediately adjacent to U.S. Highway 42 on the southwest corner of the Ghent power plant site. Disposal of ash into the 120-acre pond began when the Ghent power plant became operational in 1973 and continued over a period of 20 years until the upper ash pond became operational in 1993. The Ghent power plant has four separate generating units. Units 1 and 2 burn a high sulfur coal and an Appalachian low sulfur compliance coal. Units 3 and 4 have multi-fuel burners and are fueled by a mixture of low sulfur subbituminous and bituminous coal. The coals burned within these units were subjected to major and trace elemental analyses, mercury analysis, and loss-on-ignition (LOI) tests.

The experimental portion of this project emphasized the collection and analysis of the coal used by the Ghent power plant and the fly and bottom ashes produced during combustion. An existing technology known as vibracoring was adapted for collecting core samples from the lower ash pond. This technology enabled the collection of undisturbed ash samples from a known depth, for nearly the entire 40-foot depth of the lower pond. In all, approximately 405 feet of core was collected from 13-vibracore holes. The cores revealed layers of ash with well-preserved small scale sedimentary structures such as channel fills or gradational sequences.

Sampled cores were described visually and digitally photographed before being submitted for laboratory analyses. Laboratory characterization included an array of both physical and chemical analyses. Physical descriptions of the cored samples revealed nine sediment types: silt, sandy silt, silt and sand, sand, silty sand, gravel, silt and gravel, sand and gravel, and clay. By categorizing core descriptions using the nine sediment types, interpretations and correlations between, and surrounding, the cores were made using sedimentologic profiles (Appendix A), eliminating the need for further coring between previously cored holes. The division of cores into sedimentologic types provided 381 samples for laboratory analysis.

Dry-sieve analysis showed the ponded ash to be fine, with an average of 87.5% of the collected sample passed through a No.100-mesh sieve (150 μm). Particle-size analyses of the 381, <100-mesh fraction samples produced particle sizes that averaged between 13 μm and 99 μm . The mean particle size of the ash decreases with increasing distance from the slurry input point. LOI analyses of the 762 <100- and >100-mesh fractions of ash show an increase in LOI as the particle-size diameters increase. LOI percentages for the <100-mesh fraction range from 1.3% to 10.1%. The majority of unburned carbon resides in the coarse, >100-mesh fraction of ash with LOI's ranging from 2.0% to 56.6%. A compilation of the laboratory-analysis data and field data for each of the 13 cores can be found in Appendix B.

A mineralogical and chemical analysis of the core samples retrieved from the ash pond included x-ray diffraction (XRD), x-ray fluorescence (XRF), and a petrographic analysis using a 50x-oil objective with a reflected light microscope. Fly ash and bottom

ash are comprised of inorganic and organic constituents. The inorganic part consists mainly of amorphous components (glass spheres, spheroids, angular and irregular particles) and lesser amounts of crystalline components. The typical crystalline components included quartz, magnetite, hematite, mullite, feldspars, gypsum, anhydrite, kaolinite-metakaolinite, Ca-Mg silicates, lime, portlandite, and cristobalite. Less common minerals included mica, calcite, olivine, spinel, maghemite, limonite, magnesioferrite, Fe, Na-K and Mg sulfates.

The ponded fly ash falls into the ASTM C-618 category of a Class F pozzolan. For Class F ashes, the sum total of three major oxides, silica (Si_2O_3), iron (Fe_2O_3), and alumina (Al_2O_3), must be greater than 70%, and CaO is less than 5%. The sum total of the three major oxides for the Ghent ash fell within 80% to 90%; with a CaO content of less than 5%.

Cores revealed layers of ash with colors varying from tan to dark gray. The color of fly ash varies depending on its chemical and mineral constituents before, and after, weathering processes. The four most common colors were brown, tan, dark gray, and light gray. The primary oxides detected were quartz, aluminosilicate glass, hematite, anhydrite, and mullite. An abundance of a particular oxide in the ash is the likely reason for the various observed colors. Petrographic analysis yielded an abundance of smooth glassy spheres in the <100-mesh, ash fraction. Intervals of unburned carbon were encountered, macroscopically and microscopically, throughout the pond. Analysis of additional samples taken from collected cores revealed microscopic coarsening-upward sequences. Also revealed were cyclic layers of carbon-poor and carbon-rich laminae and small-scale sedimentary structures.

The Ghent ash pond was mapped by recording the core-hole locations with a global-positioning system. Using ArcView GIS the core-hole locations were layered onto aerial photographs of the pond, as well as various other digitized information. Statistical contouring methods were applied to the core-hole data to show the spatial variations of the data throughout the pond. An iso-grade analysis was completed for the ash pond to map the spatial distributions of data collected from the pond core analysis. The ash pond has an approximate depth of 40 feet. Therefore eight iso-grade maps, displayed in 5-foot intervals, were compiled for the following data: weight-percent, mean-particle size, and loss-on-ignition. Iso-grade maps can be used in conjunction with reserve estimates to help target areas of the pond that may yield the highest quantity of a desired product.

A reserve estimation on the total available tons of <5 μm ash, <10 μm ash, fine carbon, and coarse carbon was performed. Following the Theissen Polygon Method, two sets of calculations were performed on the area within the perimeter of the core holes, and on the area of the entire lower pond. The entire pond has a total volume exceeding 200,000,000 ft^3 , with over 7,000,000 tons of ash. Throughout the lower pond, there is over 1,000,000 tons of <5 μm ash, over 1,800,000 tons of <10 μm ash, over 200,000 tons of fine carbon, and over 1,500,000 tons of coarse carbon.

INTRODUCTION

This project will complete the final design and construction of an ash beneficiation plant that will produce a variety of high quality products including pozzolan, mineral filler, fill sand, and carbon. All of the products from the plant are expected to have value and be marketable. The ash beneficiation process uses a combination of hydraulic classification, spiral concentration and separation, and froth flotation. The advanced coal ash beneficiation processing plant will be built at Kentucky Utility's 2,200 MW Ghent Power Plant in Carrollton, Kentucky. The technology was developed at the University of Kentucky Center for Applied Energy Research (CAER) and is being commercialized by CEMEX Inc. with support from LG&E Energy, Inc., the UK CAER, and the U.S.DoE.

This technical report includes research that was conducted during the pre-award phase of the study up to December 31, 2004. It focuses on the characterization of the ash as produced by the power plant, and the ash stored in the lower pond. The objective of this effort is to provide information relative to the overall nature and quality of the ash to base processing decisions on. Key considerations include logistics and materials to feed the processing plant, as well as plant-site locations.

This work was conducted as part of the first Task of the study titled "Project Definition" which includes work to characterize the nature of the ash at Ghent (Subtask 1.1, 1.2, 1.3), work to evaluate the various units of the processing circuit (Subtask 1.4), work to evaluate the quality and value of the products from the study (Subtask 1.5), an economic assessment of the overall project (Subtask 1.5) and finally the processing plant sighting at the facility (Subtask 1.6).

EXPERIMENTAL

Ash and Coal Collection and Characterization from the Ghent Power Plant.

The coal used by the Ghent power plant and the fly and bottom ashes produced were sampled during the pre-award phase of the study. The fly ash was collected from bins that were associated with the electrostatic precipitator collection fields. The Ghent plant uses two-field ESP and the bulk of the ash is collected in the first field.

The samples were returned to the UK CAER lab. There they were subjected to ultimate and proximate analysis utilizing standard ASTM techniques. The samples were ashed and subjected to X-ray fluorescence analysis for both major and trace elements using international ash and rock standards as calibration. Mercury was analyzed on a LECO Hg analyzer on a raw sample basis.

The Coring and Analysis of Ash in the Lower Pond at Ghent.

Sampling the Ghent ash pond required the adaptation of a previously existing technology known as vibracoring (Figure 1). This was necessary to collect ash samples from the entire 40 feet depth of the pond. The Center for Applied Energy Research owns and operates an ARGO amphibious augering system. However, the sample that this augering system provided was disturbed, and the depth from which the core was taken could only be estimated. The vibracoring system provided an undisturbed sample from a known depth. This sample collection method provided the means to accurately investigate the pond samples in the laboratory.

Working within an inactive ash pond, vibracoring proved to be a more suitable method for collecting ash samples than bulk sampling, augering, or other large-coring systems. Vibracoring proved to be an inexpensive alternative to sampling pond ash, instead of using truck- or track-vehicle-mounted, rotary, hollow-stem, auger systems. In addition, this method aided the collection of undisturbed samples at known depths throughout the pond. Twenty-foot (6.1-m) lengths of core tube used in combination with a quick-release vibrator clamp reduced the amount of time spent coring nearly in half.

Analysis of the cored samples included an array of laboratory tests. These tests included dry-sieve analysis, laser particle-size analysis, loss-on-ignition, x-ray diffraction, x-ray fluorescence, and petrographic analysis. All of the data collected from these tests were compiled into spreadsheets with Microsoft Excel; an example is shown in Table 1.



Figure 1. Photo of Argo with Vibracore Apparatus.

Table 1. An example of the spreadsheet created in Microsoft Excel used to compile the data collected from each vibracore hole.

Hole #	Avg Depth	Avg Depth	Weight (g)		Weight %		Mean (µm)	% LOI		Saturation	<5 µm	<10 µm
	(feet)	(meters)	<100	>100	<100	>100	<100	<100	>100	Level	%	%
VH-16	0.7	0.20	680	44	93.9	6.1	52.72	2.0	14.4	dry	10.0	18.3
VH-16	1.9	0.57	399	297	57.3	42.7	58.16	2.2	2.5	dry	9.2	16.5
VH-16	3.0	0.91	549	219	71.5	28.5	54.81	3.1	7.5	dry	10.1	18.4
VH-16	4.8	1.46	834	92	90.1	9.9	41.18	3.1	7.7	moist	15.6	28.0
VH-16	8.0	2.44	2167	184	92.2	7.8	35.35	5.0	18.5	moist	15.9	29.6
VH-16	10.5	3.19	557	38	93.6	6.4	49.39	3.7	8.5	moist	17.1	30.7
VH-16	11.5	3.49	160	33	82.9	17.1	89.59	1.6	10.2	dry	3.5	6.3
VH-16	12.3	3.73	192	96	66.7	33.3	43.76	3.7	8.5	moist	14.8	27.0
VH-16	12.8	3.89	247	18	93.2	6.8	50.59	6.1	19.5	moist	9.8	20.4
VH-16	13.4	4.09	787	12	98.5	1.5	35.71	4.2	25.9	moist	14.3	27.3
VH-16	14.5	4.43	443	160	73.5	26.5	80.64	3.8	4.2	moist	10.3	18.9
VH-16	16.3	4.97	1134	16	98.6	1.4	29.57	3.7	39.4	wet	17.0	31.4
VH-16	18.1	5.51	693	67	91.2	8.8	47.42	4.7	29.8	wet	9.8	19.5
VH-16	19.3	5.88	358	49	88.0	12.0	59.90	4.1	22.6	moist	9.1	17.9
VH-16	20.3	6.20	564	51	91.7	8.3	52.29	3.7	16.1	moist	9.4	17.6
VH-16	21.5	6.57	631	14	97.8	2.2	36.90	1.7	14.8	wet	13.8	26.1
VH-16	22.8	6.93	445	9	98.0	2.0	83.45	3.4	13.1	moist	7.0	13.1
VH-16	24.0	7.33	548	12	97.9	2.1	39.46	2.4	21.6	dry	13.8	26.0
VH-16	25.6	7.80	767	27	96.6	3.4	49.85	2.5	25.4	wet	10.5	19.6
VH-16	27.3	8.31	795	3	99.6	0.4	28.89	1.9	21.7	wet	17.1	32.1
VH-16	28.9	8.80	781	4	99.5	0.5	26.05	1.8	16.5	wet	19.1	35.3
VH-16	30.2	9.21	923	3	99.7	0.3	26.73	3.1	15.6	wet	18.0	33.9
VH-16	31.9	9.72	1382	9	99.4	0.6	20.68	1.5	14.7	wet	21.5	41.0
VH-16	33.5	10.20	752	5	99.3	0.7	39.37	1.7	13.7	moist	13.6	25.3

Pond Core Analysis

Core logging consisted of visual descriptions and digital photographs that were taken of the samples while in the field. Such logging allowed for further interpretation of the samples upon returning to the lab. Visual descriptions included type of lithology, grain size, sedimentary structures, color, and a visual description of sample saturation. Digital photographs were imported into a laptop computer, and could be accessed for immediate viewing. Data collected in the field were entered into a Microsoft Excel 2000 spreadsheet.

Cores yielded highly variable layering. The most noticeable differences between layers were the variable grain sizes and the colors of each layer. Examination of the 13 vibracores noted nine different sedimentological units based on grain-size composition. These units include: 1.) silt, 2.) sandy silt, 3.) silt and sand, 4.) sand, 5.) silty sand, 6.) gravel, 7.) silt and gravel, 8.) sand and gravel, and 9.) clay. Each type of unit is described in detail below. An example of the descriptive sedimentologic columns from the 13 vibracores, illustrating distribution of the nine units, can be found in Figure 2. The sedimentologic units were created to enable continuity between descriptions when logging core samples. In addition, the sedimentologic units made up the framework necessary to make correlations of data throughout the pond.

To understand the nature and composition of the pond ash, it was beneficial to understand the stratigraphy and sedimentation patterns within ash ponds, in order to determine the depositional patterns of the slurried ash as it enters the pond. Depositional patterns may be used to locate desired particle-sizes, avoid and/or locate high-carbon zones, and aid in recovery operations.

Sediment Types

Unit 1: Silt

Bed Thickness	Lamina to thick-bedded
Bedding	Massive to parallel-laminated; normal grading
Color	Light to dark gray; black; white
Grain Size	<1/16 mm
Sorting	Well-sorted
Roundness	Well-rounded
Sedimentary Structures	Low-angle cross beds
Comments: Silt beds in the bottom depths of the ash pond are saturated with water.	

Unit 2: Sandy Silt

Bed Thickness	Lamina to very thick-bedded
Bedding	Mostly massive, with occasional parallel-laminated sand; normal and reverse grading
Color	Light to dark gray; black; dark brown
Grain Size	<1/16 – 1/4 mm
Sorting	Well-sorted
Roundness	Sub- to well-rounded
Sedimentary Structures	low-angle cross beds, convolute bedding, flame structures
Comments: Bedding sometimes exhibits a blending of colors between laminae. Sand laminae typically consist of sand-size particles of unburned carbon.	

Unit 3: Silt and Sand

Bed Thickness	Very thin- to thick-bedded
Bedding	Normal to reverse grading; nongraded or normally graded silt; interbedded silt and sand are most common
Color	Light to dark gray; white; black
Grain Size	<1/16 – 2.0 mm
Sorting	Well- to poorly-sorted
Roundness	Sub- to well-rounded
Sedimentary Structures	Some cross beds; cut and fill
Comments: Beds of silt and sand commonly alternate with massive beds of sandy silt.	

Unit 4: Sand

Bed Thickness	Lamina to thick-bedded
Bedding	Normal and reverse grading; parallel-stratified occasionally occurring with scattered pebbles; massive bedding is rare
Color	Light to dark gray; black; white
Grain Size	Fine- to coarse-grained
Sorting	Well- to very well-sorted
Roundness	Rounded to well-rounded
Sedimentary Structures	Erosional bases; cross beds
Comments: The upper parts locally consist of cross-stratified sand, covered with cross-laminated fine sand and occasionally topped with silt.	

Unit 5: Silty Sand

Bed Thickness	Thin- to thick-bedded
Bedding	Horizontal to cross-stratified
Color	Light to dark gray; black; white; light to medium brown
Grain Size	
Sorting	Well-sorted
Roundness	Sub-rounded to well-rounded
Sedimentary Structures	Trough cross beds common, can be seen in tabular form
Comments:	

Unit 6: Gravel

Bed Thickness	Thin- to very thick-bedded
Bedding	Massive, normally graded, with uneven erosional bases
Color	Light to dark gray; black; light to dark tan; orange
Grain Size	Small pebbles to small cobbles
Sorting	Poorly to moderately sorted
Roundness	Very angular to subangular
Sedimentary Structures	Cut and fill
Comments:	Matrix is a mixture of poorly sorted sand and silt, in some cases muddy. Some of these beds occur as recognizable channel-fill bodies, less than a foot thick (0.3m). Most beds contain abundant sand- to gravel-size carbon.

Unit 7: Silt and Gravel

Bed Thickness	Very thin- to thick-bedded
Bedding	Massive, clast-supported
Color	Light to dark gray; black; light to dark tan; and orange
Grain Size	Silt to granule
Sorting	Poorly sorted
Roundness	Angular to well-rounded
Sedimentary Structures	Cross beds
Comments:	Sand-size gravel is present.

Unit 8: Sand and Gravel

Bed Thickness	Thin- to very thick-bedded
Bedding	Massive, weakly normally graded, low-angle cross- and planar parallel-stratified
Color	Light to dark gray; black; light to medium tan
Grain Size	Small cobble-bearing pebble gravel and fine- to medium-grained sand
Sorting	Moderately to well-sorted
Roundness	Angular to rounded
Sedimentary Structures	Cross beds; cut and fill
Comments: The beds have a sheet-like geometry, and their sandy upper parts commonly show a considerably wider lateral extent than the basal gravel, which pinches out more abruptly.	

Unit 9: Clay

Bed Thickness	Lamina to thin-bedded
Bedding	Planar parallel-stratified
Color	Medium to dark brown; reddish-brown
Grain Size	Extremely fine-grained
Sorting	Well-sorted
Roundness	Well-rounded
Sedimentary Structures	None
Comments: Clay intervals may exist from erosion of construction material that washed into the pond from the embankments.	

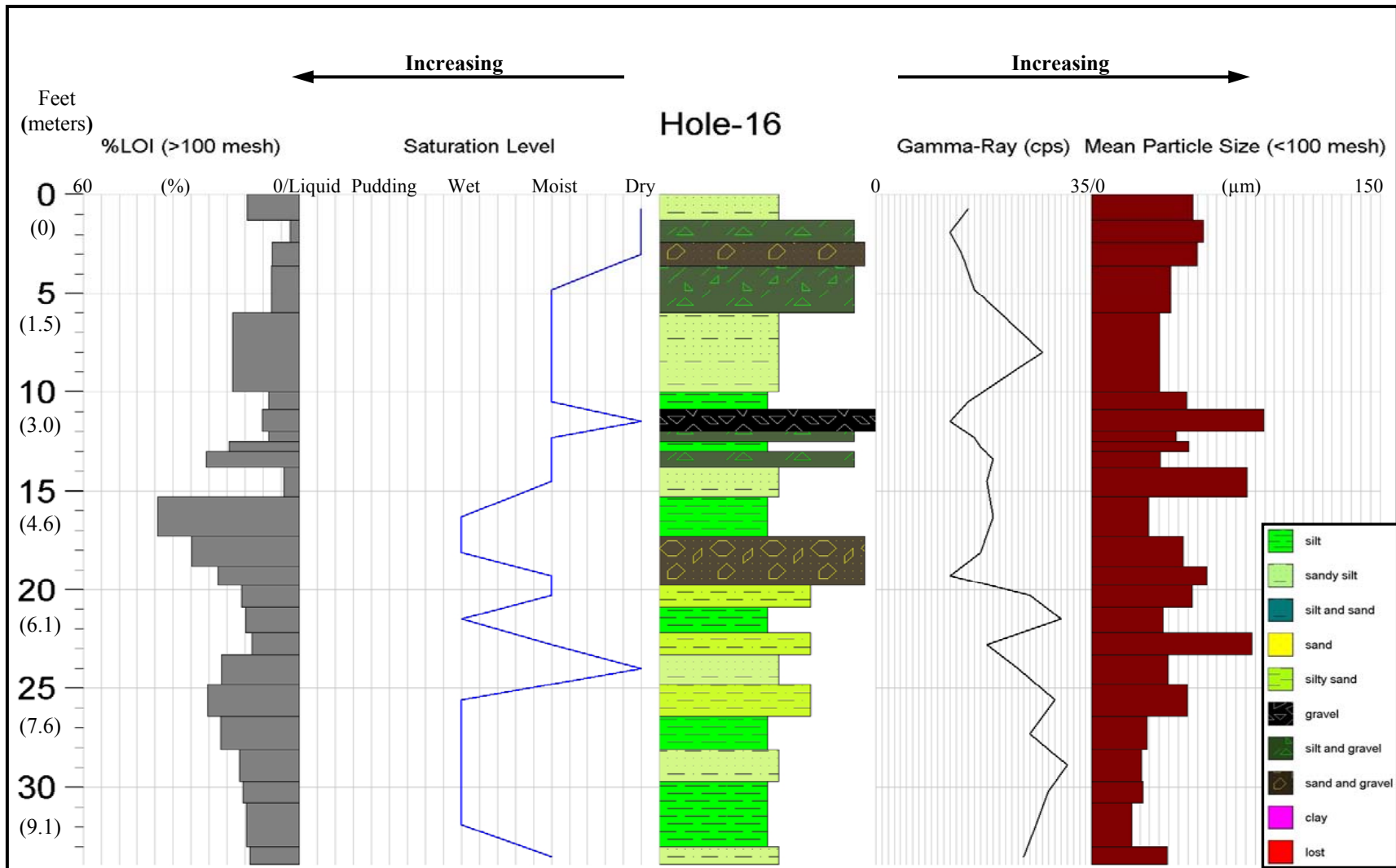


Figure 2. Sedimentologic column of vibracore-hole 16.

RESULTS AND DISCUSSION

The Ghent power plant has four separate generating units. Units 1 and 2 were part of the initial construction. Unit 1 uses high sulfur coal (Table 2) and has a forced air wet scrubber. It produces synthetic gypsum which is processed and used at a nearby wallboard plant. The Unit 2 boiler is fueled by Appalachian low sulfur compliance coal. The 3 and 4 Units, built later, have multi-fuel burners and are fueled by a mixture of low sulfur sub-bituminous and bituminous coal.

Table 2. Ultimate Analysis of Coal Used at Ghent Power Plant

Coal Type	Unit	%Ash	%C	%H	%N	%S	%O
Bituminous	1	14.54	68.07	4.85	1.17	4.57	6.80
Bituminous	2	11.95	70.61	5.07	1.25	0.61	10.51
Subbituminous	3	7.52	53.53	6.42	0.74	0.42	31.37
Bituminous	3	11.32	64.74	5.36	1.09	0.53	16.96
Subbituminous	4	7.08	52.73	6.36	0.71	0.26	32.86
Bituminous	4	13.36	70.18	4.90	1.25	0.61	9.70

The major element analysis of the ash from each of the coals used at Ghent shows some important differences (Table 3). The subbituminous coal is found to be much higher in CaO, Na₂O, K₂O and sulfate compared to the bituminous coal. The high sulfur bituminous coal is much higher in Fe₂O₃ compared to the compliance coal of Unit 2.

Table 3. Major Element Analysis of Coal Ash

Coal Type	Unit	%SiO ₂	%Al ₂ O ₃	%Fe ₂ O ₃	%CaO	%MgO	%Na ₂ O	%K ₂ O	%P ₂ O ₅	%TiO ₂	%SO ₃
Bituminous	1	46.57	20.59	22.53	2.33	0.70	0.44	2.03	0.34	1.09	1.93
Bituminous	2	56.75	28.69	5.57	1.69	1.18	0.73	2.38	0.09	1.76	1.19
Subbituminous	3	41.70	17.48	7.07	12.39	2.68	1.42	1.03	0.57	1.11	10.16
Bituminous	3	54.91	23.09	5.06	4.36	1.36	0.80	1.82	0.23	1.44	3.54
Subbituminous	4	41.89	18.03	5.04	13.47	2.98	1.52	0.92	0.62	1.11	8.17
Bituminous	4	60.09	25.31	4.04	1.40	0.86	0.27	2.12	0.09	1.57	0.87

Large differences in the trace element chemistry are not apparent (Table 4), in the coal ash analysis, with the possible exception of Ba, which is much higher in the subbituminous coal ash. Mercury concentrations in the raw coal are found to be highest in the high sulfur bituminous coal of Unit 1. On a Btu basis, however, the subbituminous coal would actually have the higher Hg emissions.

Table 4. Trace element Analysis of Coal Ash in ppm. Hg is reported on raw coal basis

Coal Type	Unit	As	Ba	Co	Cr	Cu	Mn	Mo	Ni	Pb	Sr	V	Zn	Zr	Hg
Bituminous	1	39	610	57	58	55	188	<10	<10	48	553	108	74	167	0.11
Bituminous	2	54	792	37	72	165	226	29	72	33	636	192	95	329	0.06
Subbituminous	3	26	3376	23	75	133	118	19	113	35	1794	246	108	264	0.07
Bituminous	3	37	1795	28	59	169	96	31	178	32	1102	191	138	310	0.05
Subbituminous	4	9	3678	17	75	150	89	3	57	30	1742	265	208	237	0.08
Bituminous	4	41	1029	27	61	152	122	24	56	26	676	180	100	303	0.04

The ultimate analysis along with percent ash and loss on ignition (LOI) for the fly ashes collected from the various bins from each electrostatic precipitator field (ESP) is presented in Table 5. Unit 1 was found to produce an ash that is lowest in LOI, which meets ASTM C-618 limits of 6% for ash utilization. Units 2, 3 and 4 all have LOI which exceed 6%. In general, LOI and carbon were found to be correlated in most Class F ashes. But in the ashes from Units 3 and 4, there was a significant difference between carbon and LOI. This is most likely due to the presence of anhydrite, as indicated by the higher concentrations of sulfate sulfur (SO₃) in these ashes (Table 6).

Table 5. Ultimate, Ash and LOI analysis of Ghent Fly Ash by ESP Field.

Unit	ESP	%Ash	%LOI	%C	%H	%N	%S	%O
1	1	99.04	0.96	0.40	<0.01	<0.01	0.01	0.55
1	1	98.08	1.92	1.57	<0.01	<0.01	0.15	0.20
1	1	96.82	3.18	2.26	<0.01	<0.01	0.28	0.64
1	2	98.03	1.97	0.74	0.05	<0.01	0.56	0.62
1	2	96.40	3.60	1.99	0.07	<0.01	0.57	0.97
2	1	94.27	5.73	5.10	<0.01	0.01	0.02	0.60
2	1	93.02	6.98	5.71	0.03	0.03	0.05	0.26
2	1	94.75	5.25	4.80	0.08	<0.01	0.04	0.33
2	1	95.51	4.49	3.83	0.04	<0.01	0.06	0.56
2	2	94.03	5.97	5.22	0.10	0.01	0.15	0.49
2	2	94.65	5.35	4.13	<0.01	0.01	0.20	1.01
2	2	93.66	6.34	4.98	0.04	0.02	0.14	1.16
2	2	95.30	4.70	3.61	0.14	0.01	0.04	0.90
3	1	91.23	8.77	8.14	<0.01	0.07	0.04	0.52
3	1	93.40	6.60	6.07	<0.01	0.04	0.24	0.25
3	1	93.55	6.45	5.33	0.03	0.02	0.08	0.99
3	1	93.67	6.33	4.79	0.06	0.03	0.10	1.35
3	2	93.14	6.86	4.93	0.03	0.02	0.30	1.58
3	2	94.82	5.18	3.99	<0.01	0.03	0.15	1.01
3	2	94.58	5.42	3.35	0.03	<0.01	0.36	1.68
3	2	95.04	4.96	2.12	0.02	<0.01	0.44	2.38
4	1	93.06	6.94	6.29	0.01	0.04	0.02	0.58
4	1	94.78	5.22	4.07	0.06	0.03	0.11	0.95
4	2	94.75	5.25	2.40	0.07	0.01	0.57	2.20
4	2	93.12	6.88	4.06	0.08	0.02	0.42	2.30

The major element chemistry for the fly ashes from the various units at Ghent show interesting differences. The ash produced by Unit 1 was very high in Fe₂O₃, by a factor of four over the other ashes of the study. The Unit 2 ash was found to have very high Al₂O₃ and SiO₂ contents. The chemistry of the ash from Units 3 and 4, have substantially higher CaO and alkalis, Na₂O and K₂O which are undoubtedly contributed by the subbituminous coal component of the fuel for these units.

Table 6. Major Element Oxide Data for Fly Ash Samples by Unit and ESP Field.

Unit	ESP	%SiO ₂	%Al ₂ O ₃	%Fe ₂ O ₃	%CaO	%MgO	%Na ₂ O	%K ₂ O	%P ₂ O ₅	%TiO ₂	%SO ₃
1	1	46.12	21.09	23.81	3.07	0.71	0.46	2.08	0.39	1.11	0.30
1	1	45.62	20.97	24.01	2.99	0.70	0.46	2.09	0.41	1.10	0.31
1	1	48.23	21.03	19.15	3.01	0.80	0.57	2.37	0.54	1.17	0.42
1	2	49.09	23.83	17.40	2.99	0.88	0.58	2.53	0.68	1.25	0.70
1	2	48.88	22.10	17.86	3.03	0.86	0.59	2.47	0.63	1.23	0.63
2	1	60.22	29.01	4.54	0.90	0.82	0.88	2.53	0.09	1.75	<0.1
2	1	59.94	29.18	4.44	1.01	0.83	0.84	2.53	0.09	1.74	<0.1
2	1	58.88	29.20	4.69	1.07	0.85	0.85	2.51	0.10	1.74	<0.1
2	1	59.09	29.20	4.27	1.00	0.85	0.93	2.56	0.10	1.77	<0.1
2	2	57.73	30.02	4.63	1.14	0.91	1.05	2.70	0.14	1.79	0.03
2	2	57.34	30.53	4.52	1.18	0.96	1.09	2.75	0.16	1.80	0.05
2	2	57.96	30.09	4.68	1.09	0.91	1.00	2.72	0.14	1.78	0.02
2	2	56.93	30.60	4.52	1.19	0.94	0.99	2.81	0.16	1.81	0.06
3	1	59.81	29.39	4.86	1.20	0.88	0.29	2.59	0.11	1.75	0.02
3	1	59.45	29.76	4.53	1.20	0.89	0.30	2.61	0.11	1.76	0.06
3	1	54.79	23.43	1.72	6.57	1.76	0.96	1.69	0.31	1.48	0.56
3	1	54.73	23.74	4.55	7.00	1.86	1.00	1.74	0.34	1.50	0.55
3	2	55.75	29.63	5.11	2.59	1.19	0.40	2.62	0.27	1.79	0.46
3	2	55.58	29.74	5.05	1.54	0.99	0.33	2.71	0.20	1.81	0.11
3	2	50.41	23.33	5.66	7.78	2.13	1.05	1.78	0.43	1.45	1.45
3	2	48.66	24.53	4.93	8.69	2.30	1.17	1.82	0.58	1.52	1.85
4	1	56.92	23.63	4.54	5.18	1.52	0.60	1.72	0.21	1.46	0.22
4	1	55.84	23.72	4.55	6.31	1.70	0.75	1.68	0.28	1.50	0.42
4	2	48.86	24.55	4.95	8.42	2.23	0.87	1.88	0.56	1.55	2.15
4	2	54.87	26.90	5.13	8.16	2.31	0.92	2.06	0.50	1.61	2.20

The trace element data for the ash samples is presented in Table 7. A few differences are apparent. Barium for example was higher in the ash from Units 3 and 4, which is probably due to the higher Ba content in the subbituminous coal. There are interesting variations found based on the ESP field. For example, As was much higher in ash from the second ESP field by a factor of 2 to 4 in each of the units. Similar relationships are found for Zn and Cu. These elements are more labile than the others having lower melting and vaporization temperatures. They tend to collect in the cooler portions of the ESPs on ash that has a higher surface area.

Table 7. Trace Element Data for Fly Ash. All data is in ppm of ash except Hg which is on raw basis.

Unit	ESP	As	Ba	Co	Cr	Cu	Mn	Mo	Ni	Pb	Sr	V	Zn	Zr	Hg
1	1	46	632	60	59	49	220	<dl	<dl	55	642	130	80	182	0.007
1	1	57	651	61	73	65	272	<dl	6	53	609	134	85	175	0.029
1	1	133	722	50	76	78	266	5	17	63	735	170	137	204	0.096
1	2	256	855	49	58	106	236	18	40	79	804	217	186	219	0.007
1	2	229	888	49	60	90	238	16	<dl	78	792	199	171	215	0.041
2	1	44	853	31	72	139	145	40	69	23	646	192	79	375	0.004
2	1	36	862	30	57	131	100	33	29	26	608	173	74	363	0.007
2	1	40	851	31	71	140	155	24	76	30	613	186	82	339	0.005
2	1	52	872	33	57	166	104	33	38	29	649	182	87	356	0.004
2	2	90	984	39	72	202	169	38	89	37	725	224	133	345	0.024
2	2	106	1017	41	57	218	124	35	62	41	728	240	156	341	0.024
2	2	84	960	39	72	191	160	36	89	36	694	226	138	341	0.018
2	2	108	1011	40	57	217	112	36	64	43	754	238	157	336	0.021
3	1	47	925	32	72	154	165	32	66	29	660	189	87	361	0.001
3	1	51	984	32	57	164	102	30	44	32	721	193	94	357	0.002
3	1	38	2279	27	76	155	132	22	78	30	1340	217	103	322	0.000
3	1	46	2439	28	60	158	88	30	37	32	1505	246	114	341	0.001
3	2	105	1533	41	73	215	180	33	94	44	917	300	174	329	0.002
3	2	122	1207	43	73	224	188	31	99	46	808	281	180	330	0.002
3	2	80	2715	32	77	178	184	19	81	40	1400	288	148	277	0.001
3	2	107	3339	35	60	208	110	29	51	48	1720	323	205	292	0.003
4	1	18	1845	26	60	127	100	13	36	24	1124	200	77	325	0.001
4	1	33	2151	27	75	151	132	20	81	28	1291	218	93	323	0.001
4	2	131	3206	35	60	215	108	34	60	53	1738	381	206	303	0.002
4	2	110	3131	35	60	200	105	30	50	49	1757	353	178	334	0.002

In addition to the minor and trace elements listed in Table 7, the ash samples were analyzed for Cd, Rb and Sb which were generally found to have concentrations that fell below the limits of detection (i.e. 10 ppm) for the analytical techniques employed.

Samples of bottom ash were also collected from the various Ghent Units and their analysis is presented in Table 8. The bulk chemistry differs somewhat from the ash, as the effect of the subbituminous coal on the overall composition is not as evident for the ash collected from Units 3 and 4. Also the overall trace element content of the bottom ash was much lower. For example As is below the limits of detection and Hg is found to be present in concentrations of <1 to 5 parts per billion.

Table 8. Bottom Ash Analysis for Ghent Units.

Unit	1	2	3	4
%Ash	97.99	90.58	96.01	99.82
%LOI	2.01	9.42	3.99	0.18
%SiO ₂	43.72	65.52	64.22	60.58
%Al ₂ O ₃	19.9	25.42	25.67	24.24
%Fe ₂ O ₃	28.53	6.13	5.69	4.97
%CaO	2.47	1.05	1.20	2.78
%MgO	0.63	0.72	0.79	1.10
%Na ₂ O	0.37	0.63	0.24	0.34
%K ₂ O	1.79	2.17	2.16	1.98
%P ₂ O ₅	0.25	0.07	0.08	0.11
%TiO ₂	1.06	1.70	1.55	1.50
%SO ₃	0.11	0.02	0.02	<0.01
As	<dl	<dl	<dl	<dl
Ba	646	1016	755	1345
Co	68	26	257	25
Cr	74	75	56	76
Cu	37	101	92	86
Mn	287	208	222	158
Mo	<dl	23	17	14
Ni	2	47	11	63
Pb	46	21	20	18
Sr	507	621	495	870
V	106	152	135	167
Zn	35	35	41	36
Zr	149	372	340	352
Hg	0.009	0.005	0.001	0.000

The Characterization and Assessment of the Lower Ash Pond.

Introduction.

The lower ash pond at the Ghent station was in service for approximately 20 years. The bulk of the ash in the lower pond was derived from Units 1 and 2, but some ash from Units 3 and 4 is also present. The lower ash pond is large, over 100 acres in extent, with a volume that exceeds 200 million cubic feet. The resource assessment of this ash pond was something of a pioneering effort that required the development of both technology and techniques.

The Coring of the Lower Pond.

Vibracoring provides a way to collect an unbiased, representative sample that preserves small-scale sedimentary structures and distribution of ash, which ranges in size from silt-size to gravel-size particles. This method utilized a concrete vibrator to create high-frequency, low-amplitude (0.1 to 1.0 mm) vibrations that are transferred down a series of aluminum tubes (Lanesky et al., 1979; Smith, 1998; Thomas et al., 1991). Vibrations liquefy a 1-to 2-mm layer of sediment that is in contact with both the inside and outside wall of the aluminum tube, thus allowing penetration through unconsolidated sediment. The vibracore system enables the operator to extract soft-sediment cores from the entire depth of an ash pond. This sampling technique was initially developed to collect core samples from continental shelves, but was later adapted for lake-bottom sediments (Smith, 1992), swamp muds, and other water-saturated sediments.

Cored samples were removed from the deposit intact and undisturbed, whether they were 11 feet (3.4m) or 37.5 feet (11.4m) in length. Vibracores revealed layers of ash with well-preserved sedimentary features that were used to interpret how the ash was deposited. Small-scale sedimentary structures, such as channel fills or gradational sequences, are representative of the detail that was seen in the cored samples. Table 9 shows the total depth drilled for each of the 13-vibracore holes. In all, 405.3 feet of core were collected from the Ghent ash pond.

The factors that limited the depth of vibracore penetration were the level of sediment saturation and intervals of coarse sediments. Holes closest to the slurry input encountered the coarsest fractions of ash, which therefore reduced coring depths to below the average of 31.2 feet (9.5 m). Holes farthest away from the slurry input encountered a finer fraction of ash, and therefore, cores could penetrate deeper. Hole 08 was only cored to a depth of 11 feet (3.4 m), because at that depth the ash was in a liquid state and could not be retrieved with the core catchers. Hole 20 encountered a similar situation and 18 feet (5.5 m) of core was lost because of water-saturated ash.

Table 9. Vibracore-hole depth data.

Hole	Depth (feet)	Depth (meters)
08	11.0	3.4
09	31.0	9.4
10	37.0	11.3
11	37.4	11.4
12	34.0	10.4
13	34.6	10.5
14	37.5	11.4
15	31.4	9.6
16	33.9	10.3
17	30.1	9.2
18	35.8	10.9
19	30.2	9.2
20	21.4	6.5
Average	31.2	9.5
Sum	405.3	123.5

Dry-Sieve Analysis

The dry-sieve analysis (Figure 3) shows that an average of 87.5% of the collected sample passed through a No.100-mesh sieve, whereas 12.5% remained on the screen; demonstrating that most of the sample is a fine ash, less than 150 microns. Table 10 shows the contribution of the <100 and >100-mesh fractions of dry-sieved ash to the total weight percent for each core. Figure 4 shows the average distribution of weight percent by depth. The weight percent increases upward to approximately 20 feet (6.1 m), and then decreases toward the surface. Table 11 shows the data used to create Figure 4.

Particle-Size Analyses

The results of particle-size analyses of the 381, <100-mesh fraction, samples produced particle sizes that averaged between 13 μm and 99 μm (Figure 5). The mean particle size reflects location in the pond from which samples were collected. For example, holes 08 and 18 have the lowest mean particle sizes and were collected from the most distal (southeast end) of the pond. This is the location where the finest ash was deposited. There is also a distinct increase in mean particle size between the depths of 10 and 20 feet (3.0 - 6.1 m) (Figure 6 and Figure 7), similar to the weight-percent increase seen in Figure 4.

Loss-On-Ignition Analyses

Results for the LOI analyses of 762 core samples are shown in Figure 8, Figure 9, and Figure 10. Figure 8 shows an increase in LOI as the particle size diameters increase. As shown in Figure 9a, LOI percentages for the <100-mesh fraction range from 1.3% to 10.1%. The LOI percentages for the >100-mesh fraction range from 2.0% to 56.6% as seen in Figure 9b. Figure 10 demonstrates the relative proportions of unburned carbon in the fine- and coarse-size fractions. The majority of unburned carbon resides in the coarse, >100-mesh fraction of ash and ranges from 7.6% in Hole-20, to 29.9% in Hole-09. The LOI values for the fine, <100-mesh fraction, range from 2.4% in Hole-20, to 4.6% in Hole-12.

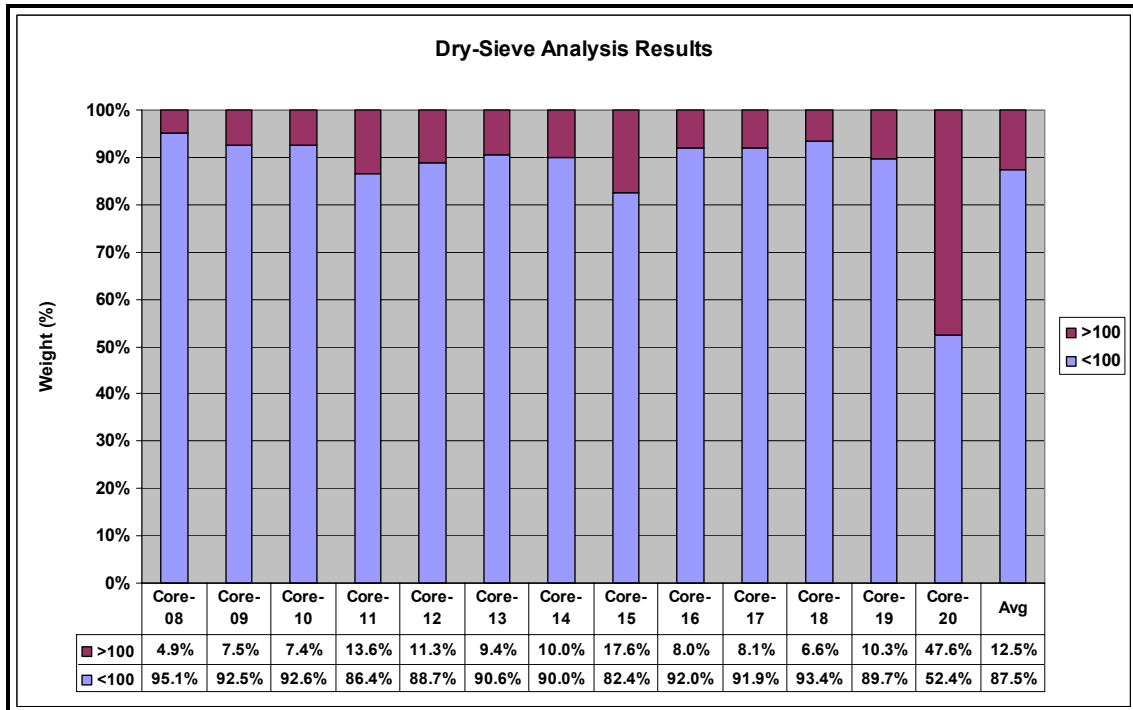


Figure 3. Dry-sieve analysis results of cored samples, showing that a majority of the sieved ash passed through the No.100 mesh.

Table 10. Dry-sieve analysis results using a No.100-mesh sieve.

Core #	<100 mesh (kg)	>100 mesh (kg)	Total Depth (ft)	Total Depth (m)
8	5.81	0.31	11.0	3.4
9	16.40	1.32	31.0	9.4
10	16.27	1.30	37.0	11.3
11	14.35	2.25	37.4	11.4
12	16.12	2.05	34.0	10.4
13	14.87	1.53	34.6	10.5
14	16.20	1.79	37.5	11.4
15	13.85	2.95	31.4	9.6
16	16.79	1.46	33.9	10.3
17	15.03	1.33	30.1	9.2
18	18.22	1.28	35.8	10.9
19	13.86	1.59	30.2	9.2
20	6.66	4.33	21.4	6.5
Sum	184.43	23.51	405.3	123.5
Percent	88.7%	11.3%		

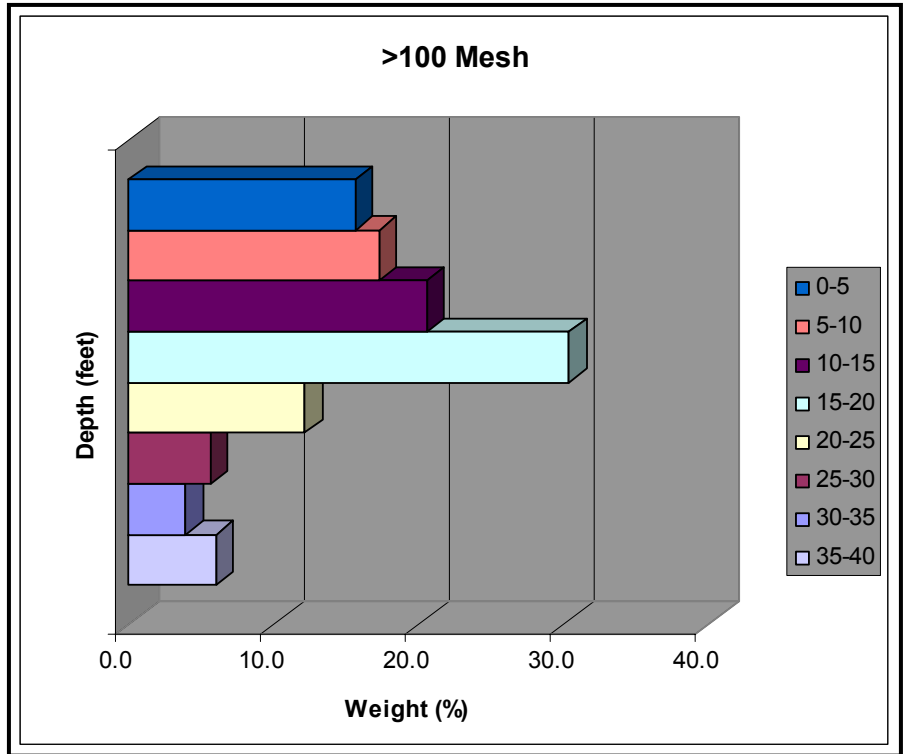


Figure 4. Chart illustrating the distribution of average weight percent for the >100 fraction of ash. Each bar represents a 5-foot (1.5-m) interval in vertical succession.

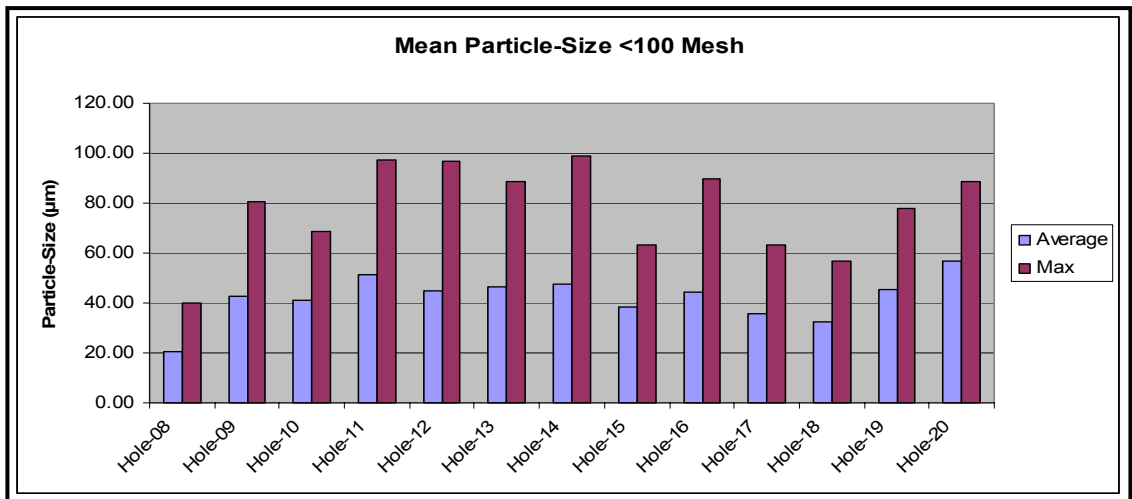


Figure 5. Mean particle-size data by hole.

Table 11. Data used to compile the bar chart in Figure 4.

Weight % (>100)		Hole 08	Hole 09	Hole 10	Hole 11	Hole 12	Hole 13	Hole 14	Hole 15	Hole 16	Hole 17	Hole 18	Hole 19	Hole 20	Average
0-5	0-1.5														
Average		43.9	3.5	9.8	5.2	4.4	3.6	3.0	32.6	21.8	7.0	1.7	6.8	60.1	15.7
5-10	1.5-3.0														
Average		18.9	5.0	6.4	6.4	5.5	10.9	3.8	45.2	8.9	20.7	19.0	23.8	50.5	17.3
10-15	3.0-4.6														
Average		6.3	23.2	21.2	12.8	20.4	16.4	24.4	21.2	15.3	17.5	12.8	27.7	48.6	20.6
15-20	4.6-6.1														
Average			26.1	20.6	65.5	57.9	32.2	55.5	32.7	26.5	4.4	4.9	24.1	13.9	30.4
20-25	6.1-7.6														
Average			4.2	3.2	19.6	18.9	8.3	13.8	32.6	3.6	3.9	1.0	3.4	33.2	12.1
25-30	7.6-9.1														
Average			2.4	8.7	16.0	5.8	3.6	6.4	12.6	1.2	1.2	1.3	2.7		5.6
30-35	9.1-10.7														
Average			0.3	2.7	1.4	8.6	12.7	2.3	1.4	0.5	0.8	5.2	7.0		3.9
35-40	10.7-12.2														
Average				1.9	1.5			2.8				17.6			6.0

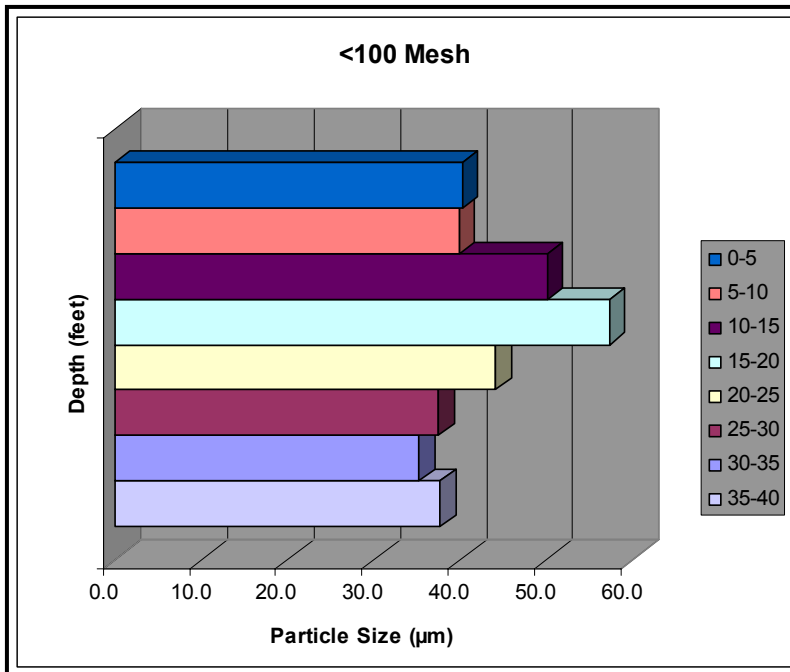


Figure 6. Chart illustrating average particle-size distribution of the <100 fraction of ash, in 5-foot (1.5-m) intervals.

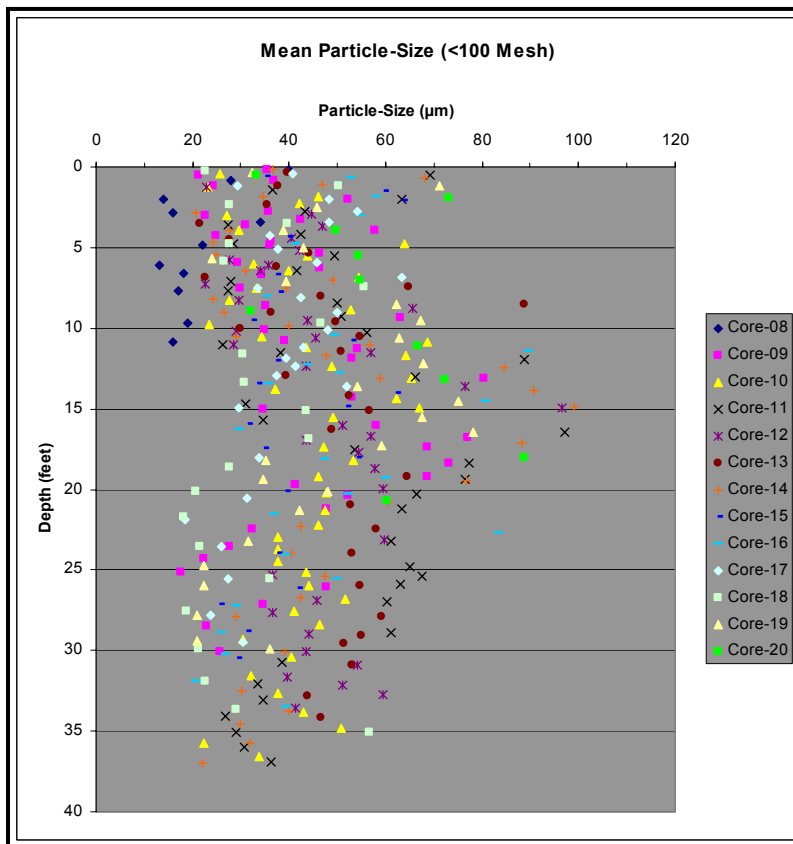


Figure 7. Scatter plot of the mean particle size for the <100 fraction of samples analyzed.

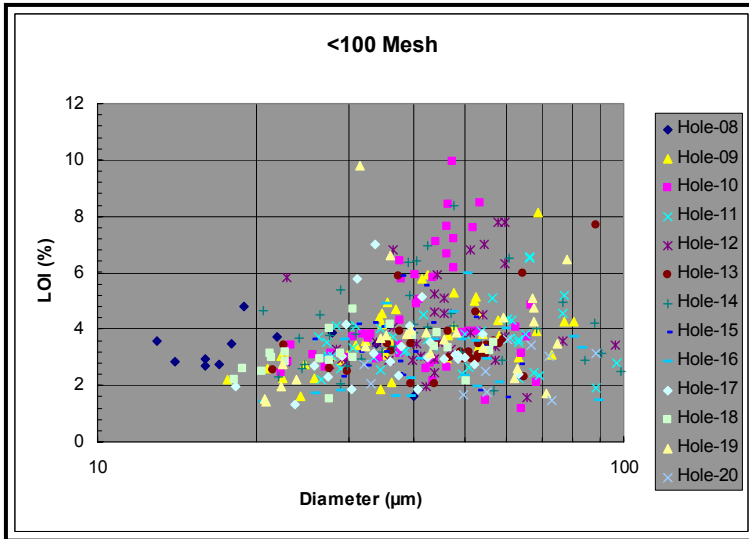


Figure 8. Loss-on-ignition data for each of the cored holes, plotted as a function of mean particle size for the <100 mesh fraction.

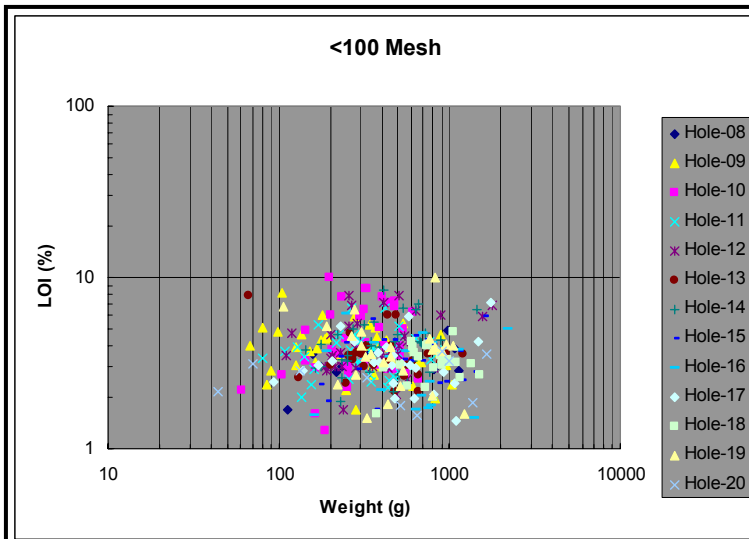
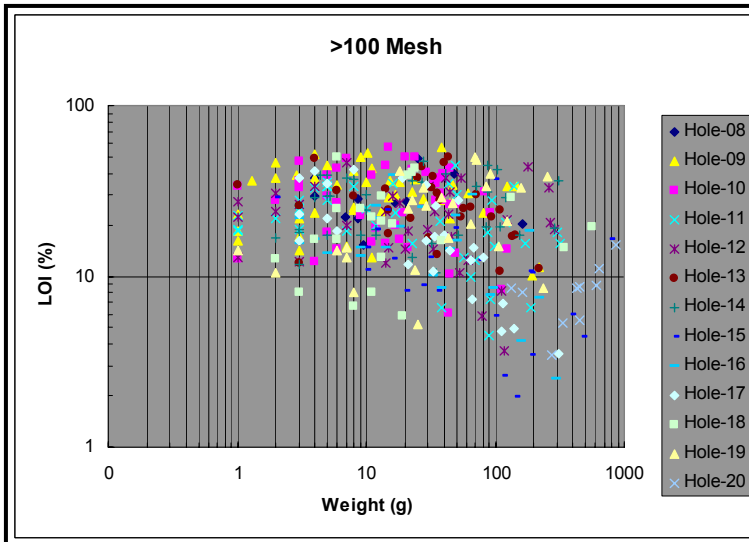


Figure 9. Loss-on-ignition data displayed as a function of sample weight: A) values for the silt to fine-sand fraction; B) values for the medium-sand to coarse-gravel fraction.



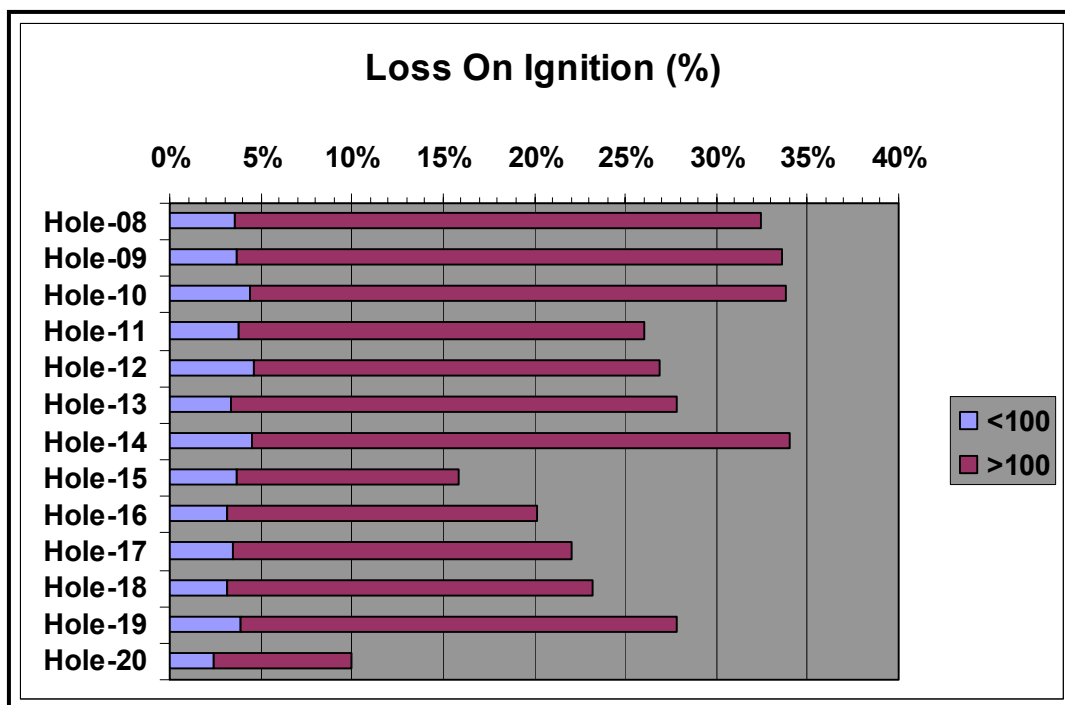


Figure 10. Average percentages of unburned carbon for the <100-mesh and >100-mesh size-fractions.

Mineralogical and Chemical Analysis.

When fly ash and bottom ash leave the high-temperature zone in boilers, they experience sharp phase transitions, which lead to intensive glass formation and limited mineral crystallization (Vassilev and Vassileva, 1996). The mineral formation results from crystal growth in silicate melts (quartz, mullite, magnetite), recrystallization (clay minerals and oxides), and solid-phase reactions (Ca – Mg silicates). Fly ash and bottom ash are comprised of inorganic and organic constituents. The inorganic part consists mainly of non-crystalline (amorphous) components (glass spheres, spheroids, angular and irregular particles) and lesser amounts of crystalline components represented by various major (quartz, magnetite, hematite, mullite, feldspars, gypsum, anhydrite, kaolinite-metakaolinite, Ca-Mg silicates, lime, portlandite, cristobalite), and minor (mica, calcite, olivine, spinel, maghemite, limonite, magnesioferrite, Fe, Na-K and Mg sulphates) mineral phases (Table 12).

Table 12 shows two classes of fly ash, Class F and Class C, and their corresponding oxide constituents. The ponded fly ash is considered to be a Class F ash. For these ashes, the sum total of three major oxides, silica (Si_2O_3), iron (Fe_2O_3), and alumina (Al_2O_3), is greater than 70%, and CaO is less than 5%, which is specified in ASTM C-618 (Table 13).

Cores retrieved from the ash pond revealed layers of ash with colors varying from tan to dark gray. The color of fly ash varies depending on its chemical and mineral constituents before, and after, weathering processes (ACAA, 2003). The four most common colors were brown, tan, dark gray, and light gray. Analyses of ash with these colors were performed with x-ray diffraction (XRD) and x-ray fluorescence (XRF) to determine the mineralogical and oxide composition of the ash. An abundance of a particular oxide in the ash is the likely reason for the various observed colors. The oxide phases seen in the sampled fly ash are listed in Table 6. The primary oxides detected were quartz, aluminosilicate glass, hematite, magnetite, anhydrite, and mullite (Figure 11 to Figure 14).

Bottom ash samples were not analyzed because they do not show great qualitative differences from fly ash with regard to the phase composition and particle morphology. The content of the amorphous and partially unburned components in bottom ash is always higher than in fly ash. Bottom ash is occasionally enriched in clay minerals, quartz, mica, feldspars and other unmelted mineral aggregates. Bottom ash demonstrates increased concentrations of Fe^{2+} glass phases and mineral species due to the more reducing conditions during bottom-ash formation (Vassilev and Vassileva, 1996).

Table 12. Typical chemistry of coal fly ash (in weight percent) (ACAA, 2003).

(%)	Class F		Class C	
	Low – Fe	High – Fe	High – Ca	Low – Ca
SiO ₂	46-57	42-54	25-42	46-59
Al ₂ O ₃	18-29	16.5-24	15-21	14-22
Fe ₂ O ₃	6-16	16-24	5-10	5-13
CaO	1.8-5.5	1.3-3.8	17-32	8-16
MgO	0.7-2.1	0.3-1.2	4-12.5	3.2-4.9
K ₂ O	1.9-2.8	2.1-2.7	0.3-1.6	0.6-1.1
Na ₂ O	0.2-1.1	0.2-0.9	0.8-6.0	1.3-4.2
SO ₃	0.4-2.9	0.5-1.8	0.4-5.0	0.4-2.5
LOI	0.6-4.8	1.2-5.0	0.1-1.0	0.1-2.3
TiO ₂	1-2	1-1.5	<1	<1

Table 13. XRF data from the analyses, on core samples, that represent the four typical colors of fly ash.

(%)	Color			
	Brown	Tan	Dark Gray	Light Gray
SiO ₂	40.85	51.13	53.97	53.27
Al ₂ O ₃	18.68	27.23	26.73	27.41
Fe ₂ O ₃	21.8	7.27	5.08	4.84
CaO	5.05	1.61	1.35	1.3
MgO	1.02	0.84	1.02	1.02
Na ₂ O	0.54	0.46	0.26	0.35
K ₂ O	2.45	1.81	2.47	2.65
P ₂ O ₅	0.23	0.26	0.2	0.21
TiO ₂	1.11	1.91	1.77	1.76
SO ₃	0.8	<0.01	0.02	<0.01
LOI	3.7	1.8	7.2	2.6
Ash	96.07	98.15	92.91	97.33
Total (SiO₂, Al₂O₃, Fe₂O₃)	81.33%	85.63%	85.78%	85.52%

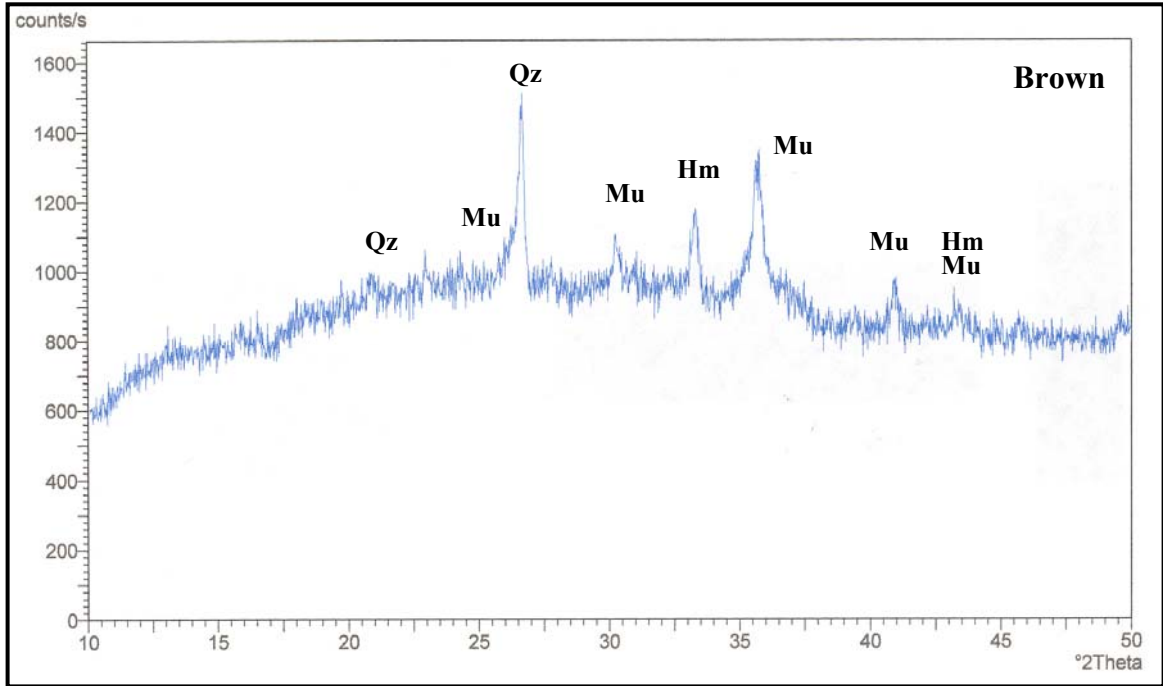


Figure 11. Diffractogram of a brown ash from hole 15, at a depth of 26.3 to 28 feet (8.0 - 8.5 m). The large arch-shaped background intensity is a product of amorphous glass in the fly ash. Qz: quartz, Mu: mullite, Hm: hematite.

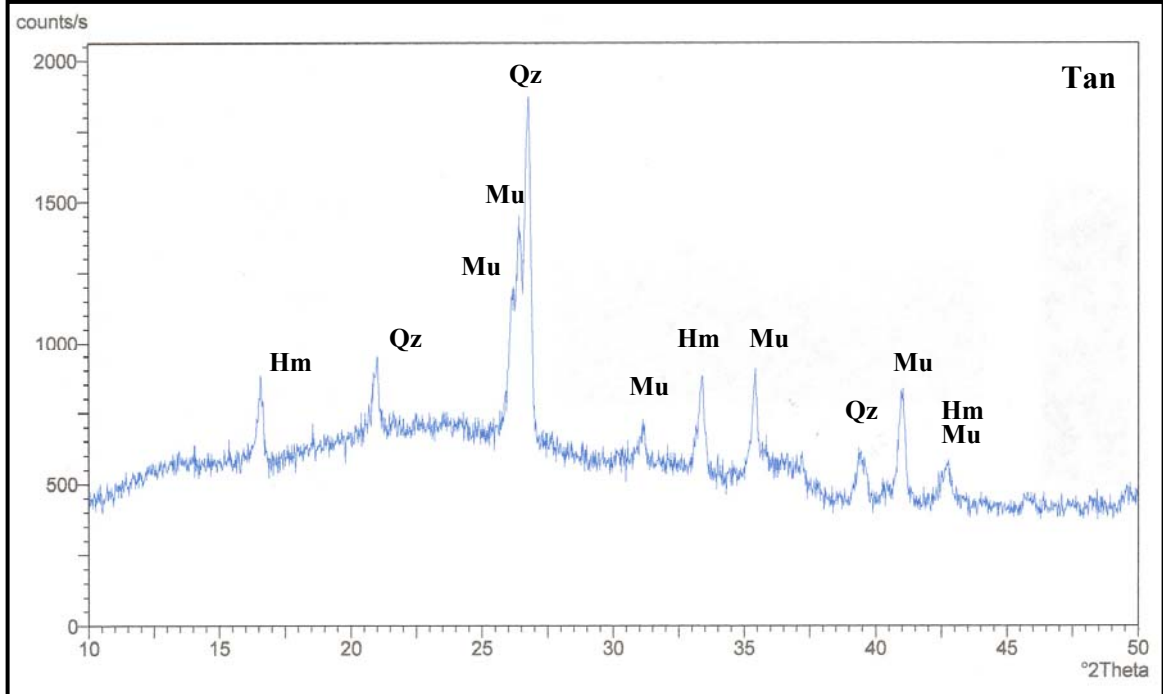


Figure 12. Diffractogram of a tan ash from hole 16 at a depth of 28.1 to 29.7 feet (8.6 - 9.1 m). Qz: quartz, Mu: mullite, Hm: hematite.

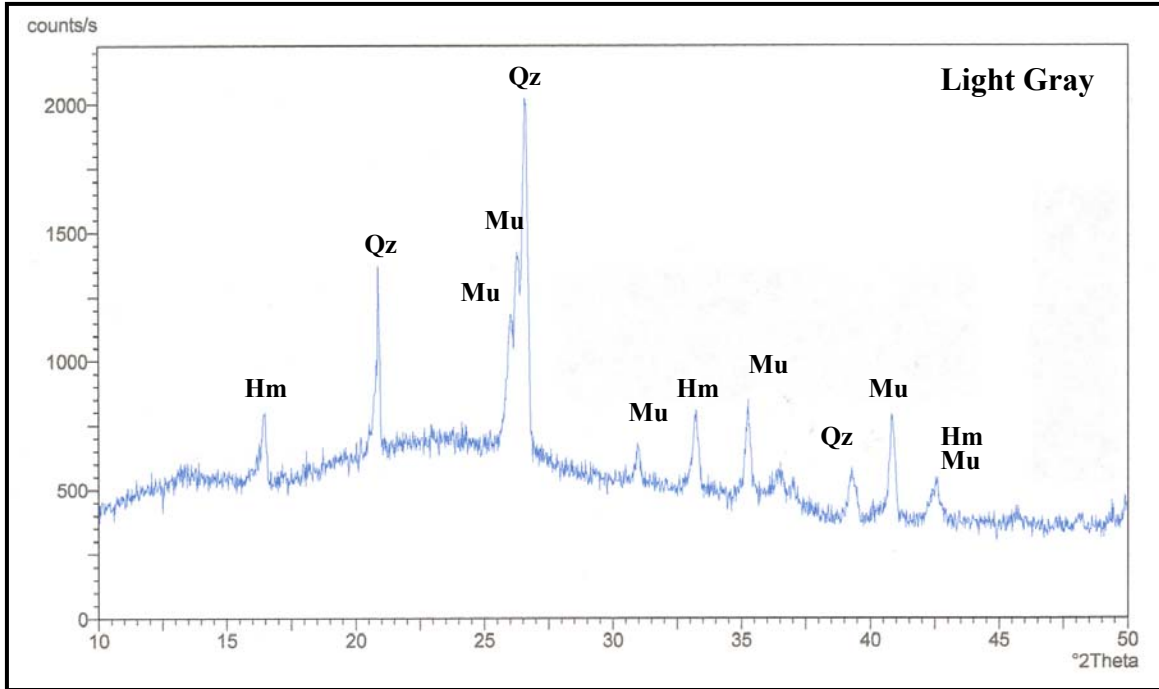


Figure 13. Diffractogram of a light-gray ash from hole 10 at a depth of 25.2 to 26.5 feet (7.7 - 8.1 m). Qz: quartz, Mu: mullite, Hm: hematite.

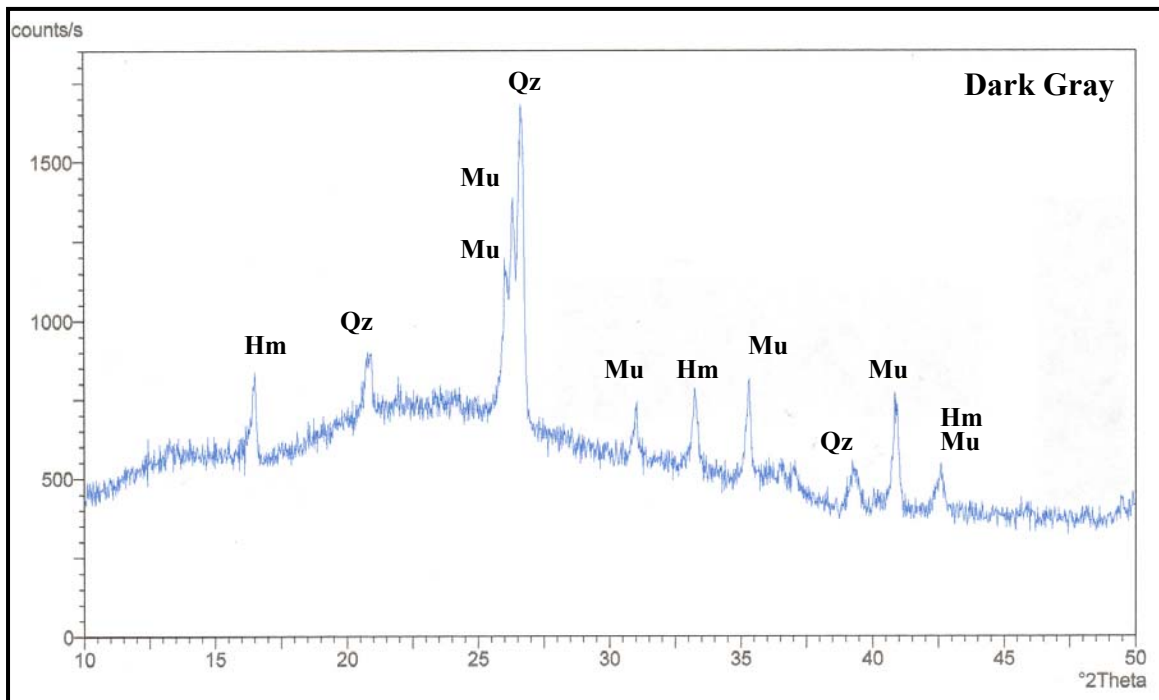


Figure 14. Diffractogram of a dark-gray ash from hole 18 at a depth of 19.1 to 21.2 feet (5.8 - 6.5 m). Qz: quartz, Mu: mullite, Hm: hematite.

Petrographic analysis yielded an abundance of smooth glassy spheres in the <100-mesh, ash fraction (Figure 15). Intervals of unburned carbon were encountered throughout the pond. One example of a typical carbon particle encountered is pictured in Figure 16. Analysis of additional samples collected from Holes 19 and 20 revealed microscopic coarsening-upward sequences (Figure 17). Also revealed were cyclic layers of carbon-poor and carbon-rich laminae and small-scale sedimentary structures (Figure 18).



Figure 15. Petrographic image of glassy fly-ash particles. Particles in this view are generally less than 20 microns in diameter. Magnification is 500x with a 50x objective in oil. This sample was taken from Hole 20 at a depth of approximately 13 feet (4 m).

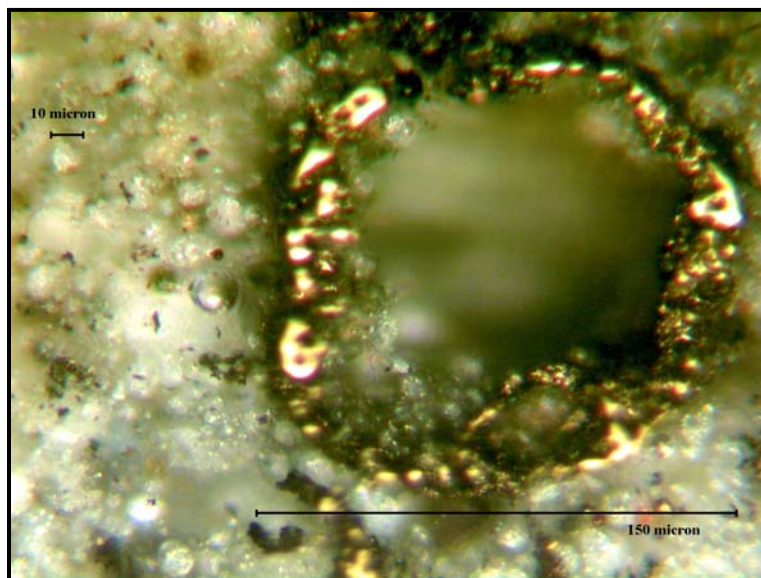


Figure 16. Petrographic image of a sand-size carbon particle surrounded by <math><10\ \mu\text{m}</math>, glassy, fly-ash spheres. Photo taken immersed in oil under 500x magnification. This sample was taken from Hole 20 at a depth of approximately 13 feet (4 m).



Figure 17. Microscopic image of a coarsening-upward fly-ash interval. The linear feature is a piece of graphical tape that measures 1/64 inches (0.4 mm) in width. The dark particles are unburned carbon.



Figure 18. Microscopic image of cyclic laminae and small-scale sedimentary structures. The light and dark layers at the bottom portion of the image are carbon-poor and carbon-rich, respectively. Above this begins a coarsening-upward sequence with planar cross-beds in a small ripple. The linear at the top of the image is a piece of graphical tape, measuring 1/64 inches (0.4 mm) in width.

Pond Mapping

The Ghent ash pond was mapped by recording the core-hole locations with a global-positioning system, or GPS. The GPS coordinates were then transferred to ArcView GIS (Figure 19). The core-hole locations were layered onto aerial photographs of the pond, as well as various other digitized information. Statistical contouring methods were applied to the core-hole data to show the spatial variations of the data, throughout the pond (Figure 20).



Figure 19. Vibracore-hole location map.

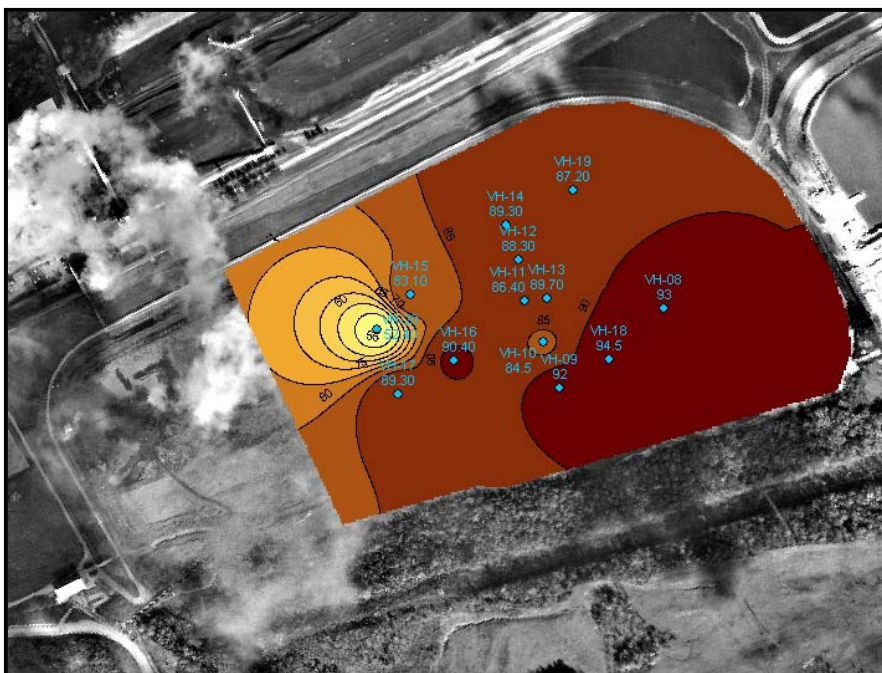


Figure 20. Example of map of <100 mesh isograds created using statistical contouring methods.

Iso-Grade Analysis

An iso-grade analysis was completed for the ash pond to map the spatial distributions of data collected from the pond core analysis. The ash pond has an approximate depth of 40 feet. Therefore eight iso-grade maps, displayed in 5-foot intervals, were compiled for the following data: weight-percent, mean-particle size, and loss-on-ignition. An example of an iso-grade map similar to those produced for the iso-grade analysis is shown in Figure 21. The data used to compile the iso-grade map in Figure 21 is shown in Table 14. Iso-grade maps can be used in conjunction with reserve estimates to help target areas of the pond that may yield the highest quantity of a desired product.

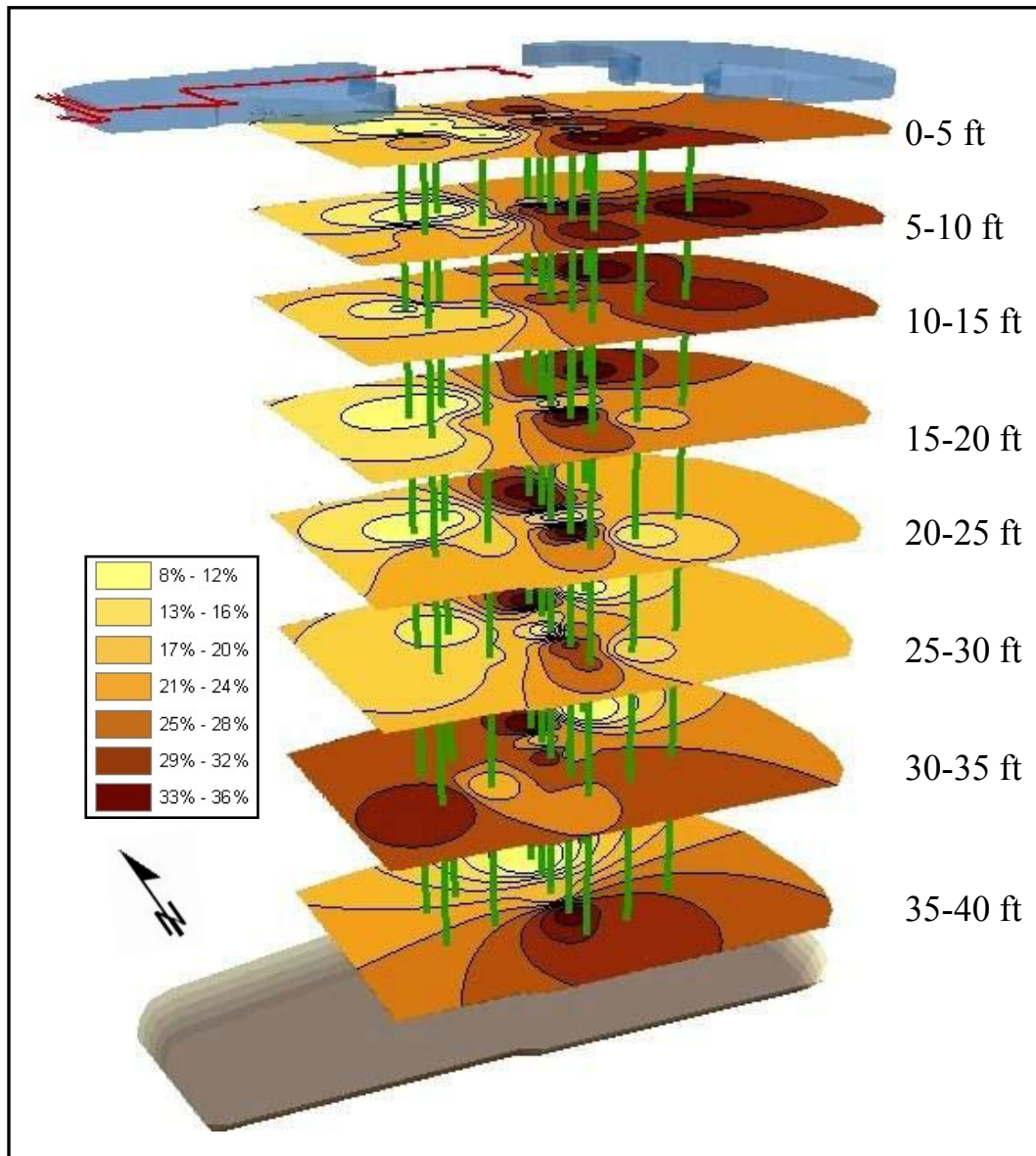


Figure 21. Stacked iso-grade maps for the average percent of unburned coarse carbon. The darker areas represent high concentrations of carbon. The vertical lines represent cored holes.

Table 14. >100-mesh, LOI data used to compile the iso-grade maps in Figure 21.

% LOI (>100)		Hole 08	Hole 09	Hole 10	Hole 11	Hole 12	Hole 13	Hole 14	Hole 15	Hole 16	Hole 17	Hole 18	Hole 19	Hole 20	Average
Depth (ft)	Depth (m)														
0-5	0-1.5														
Average		25.3	34.7	23.7	29.4	19.7	29.7	29.5	11.5	8.0	21.6	32.5	21.4	8.4	22.7
5-10	1.5-3.0														
Average		35.2	32.8	28.8	30.7	18.6	34.6	23.5	6.0	13.1	18.9	27.1	22.9	8.1	23.1
10-15	3.0-4.6														
Average		29.0	22.4	22.3	25.3	22.3	24.4	19.9	18.7	12.8	15.0	25.2	32.3	8.7	21.4
15-20	4.6-6.1														
Average			31.0	38.8	19.0	32.0	21.3	28.2	9.8	22.4	13.6	22.0	37.3	8.1	23.6
20-25	6.1-7.6														
Average			25.3	39.0	15.5	36.7	15.1	38.0	11.1	18.2	22.8	13.1	20.5	8.7	22.0
25-30	7.6-9.1														
Average			32.4	36.3	10.9	22.9	30.0	42.6	13.0	19.8	18.1	17.3	11.0		23.1
30-35	9.1-10.7														
Average			17.1	19.3	21.2	15.1	17.4	23.7	18.7	14.7	22.0	19.9	8.0		17.9
35-40	10.7-12.2														
Average				32.8	20.6			12.4				29.0			23.7

Reserve Estimation

A reserve estimation on the total available tons of ash, <5µm, <10µm, fine carbon, and coarse carbon was performed. Following the Theissen Polygon Method, the cored area was sectioned into polygons to determine the volume of ash in each polygon. The volume of each polygon was then multiplied by a tonnage factor to determine the tons of ash within each polygon. The number of tons for each polygon was then multiplied by an average grade percent to determine the number of tons of <5µm, <10µm, fine carbon, and coarse carbon. The total tons of each polygon were summed to give a total tonnage estimate for the drilled area, and the entire pond.

The drilled area has a total volume of 31,475,680 ft³, with a total of 1,056,231 tons of ash. This was determined with a tonnage factor of 29.8 ft³/ton; based on a bulk density analysis of the ash. Table 15 contains the tonnages of the <5µm ash, <10µm ash, fine carbon, and coarse carbon from within the drilled area.

Table 15. Reserve estimates for the drilled area of the pond.

Drilled Area	Tons	Average grade
<5µm Ash	158,435	15%
<10µm Ash	274,620	26%
Fine Carbon	39,081	3.7%
Coarse Carbon	232,371	22%
Fly Ash & Bottom Ash	1,056,231	-----

The entire pond has a total volume of 209,080,000 ft³, with a total of 7,016,107 tons of ash. This was determined with a tonnage factor of 29.8 ft³/ton; based on a bulk density analysis of the ash. Table 16 contains estimated tonnages of the <5µm ash, <10µm ash, fine carbon, and coarse carbon for the entire pond; based on the data for the drilled area.

Table 16. Reserve estimates for the entire pond.

Entire Pond	Tons	Average grade
<5µm Ash	1,052,416	15%
<10µm Ash	1,824,188	26%
Fine Carbon	259,596	3.7%
Coarse Carbon	1,543,544	22%
Fly Ash & Bottom Ash	7,016,107	-----

CONCLUSIONS

An examination of the ash as produced by the Ghent power plant and as stored in the lower pond, suggests that the lower ponded material is the better candidate for the feed to the beneficiation plant. There are a number of reasons for this. The ash, as currently produced is found to be highly variable. The four units at Ghent currently use high sulfur bituminous coal, a low sulfur bituminous coal and a mix of bituminous and subbituminous coals and produce ashes that are correspondingly variable.

In contrast the material in the lower pond is more homogenous and is no longer subject to change. The lower pond is also a major resource. It is projected to contain more 7 million tons of ash in a volume of over 200,000,000 ft³. The ash is capable of producing a very high grade of pozzolan, as 26% of it is finer than 10 µm. It is also a major carbon resource with almost 1.5 million tons of coarse carbon, which we consider relatively easy to recover.

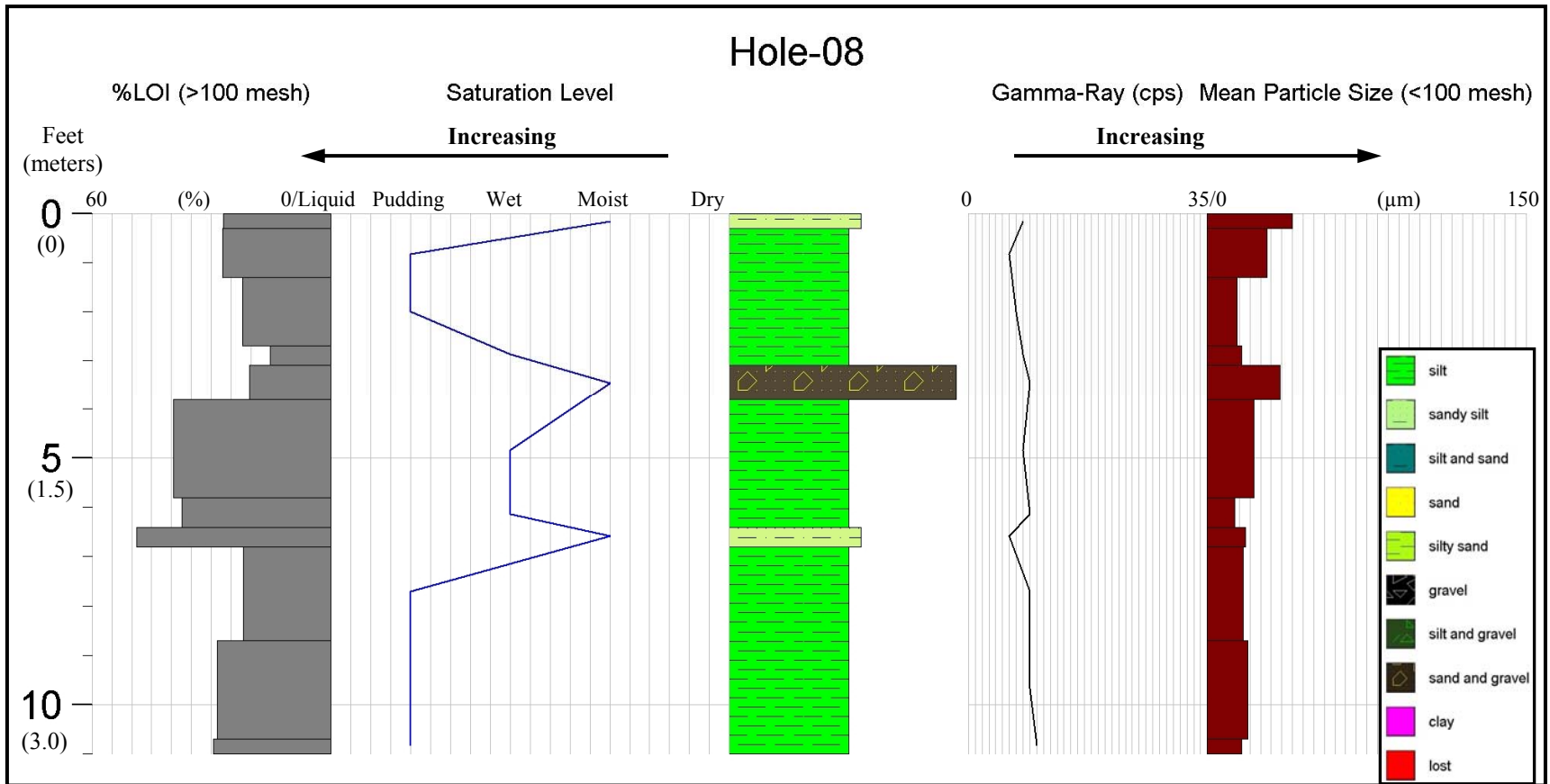
For these reasons, as well as logistical and infrastructure considerations, it is concluded that the ash beneficiation plant be constructed to be feed entirely from the lower pond. Other factors such as the distribution of the ash by size and carbon, as determined by the coring and subsequent analysis, will be taken in consideration at a later stage in our work when the actual plant site is considered.

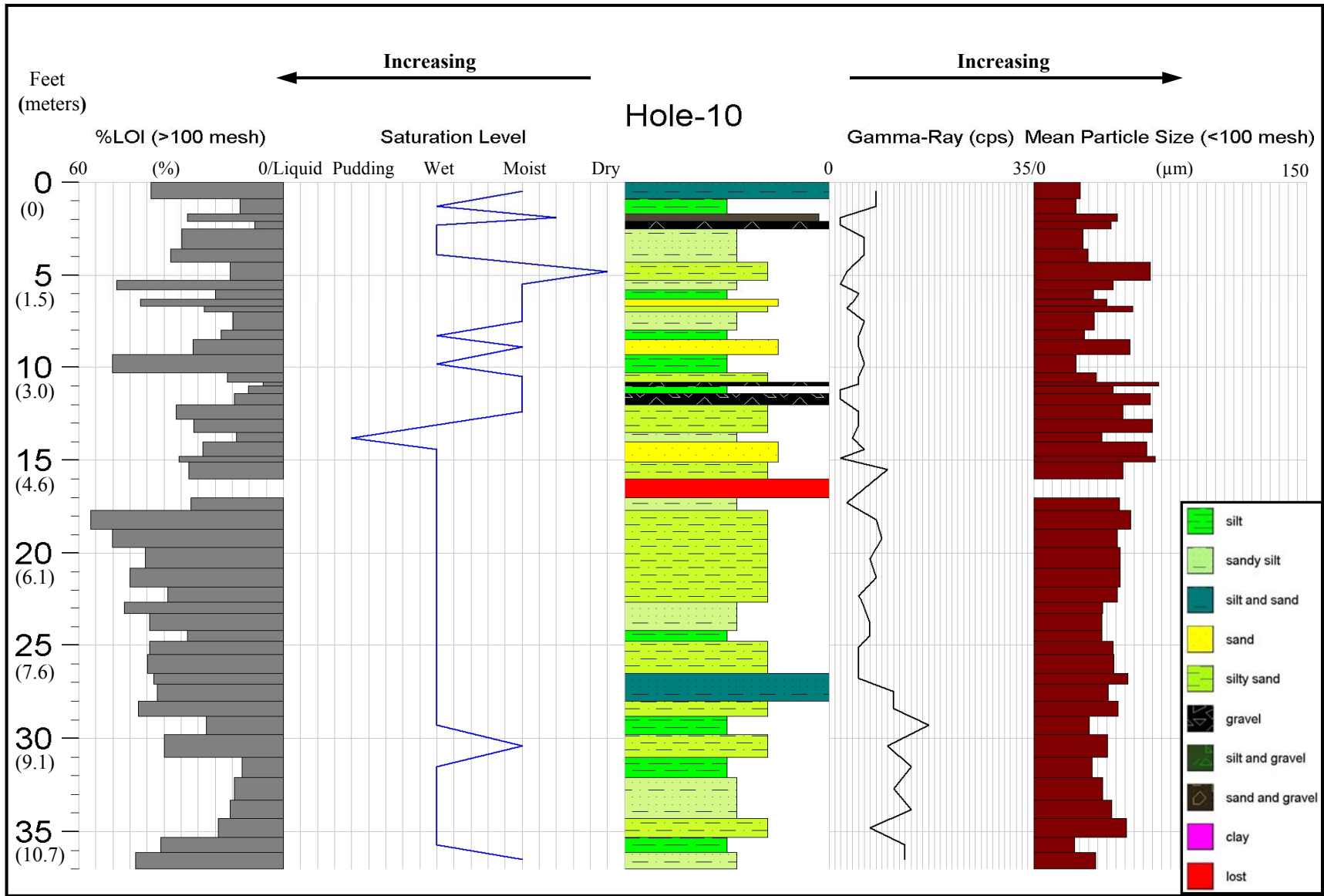
REFERENCES

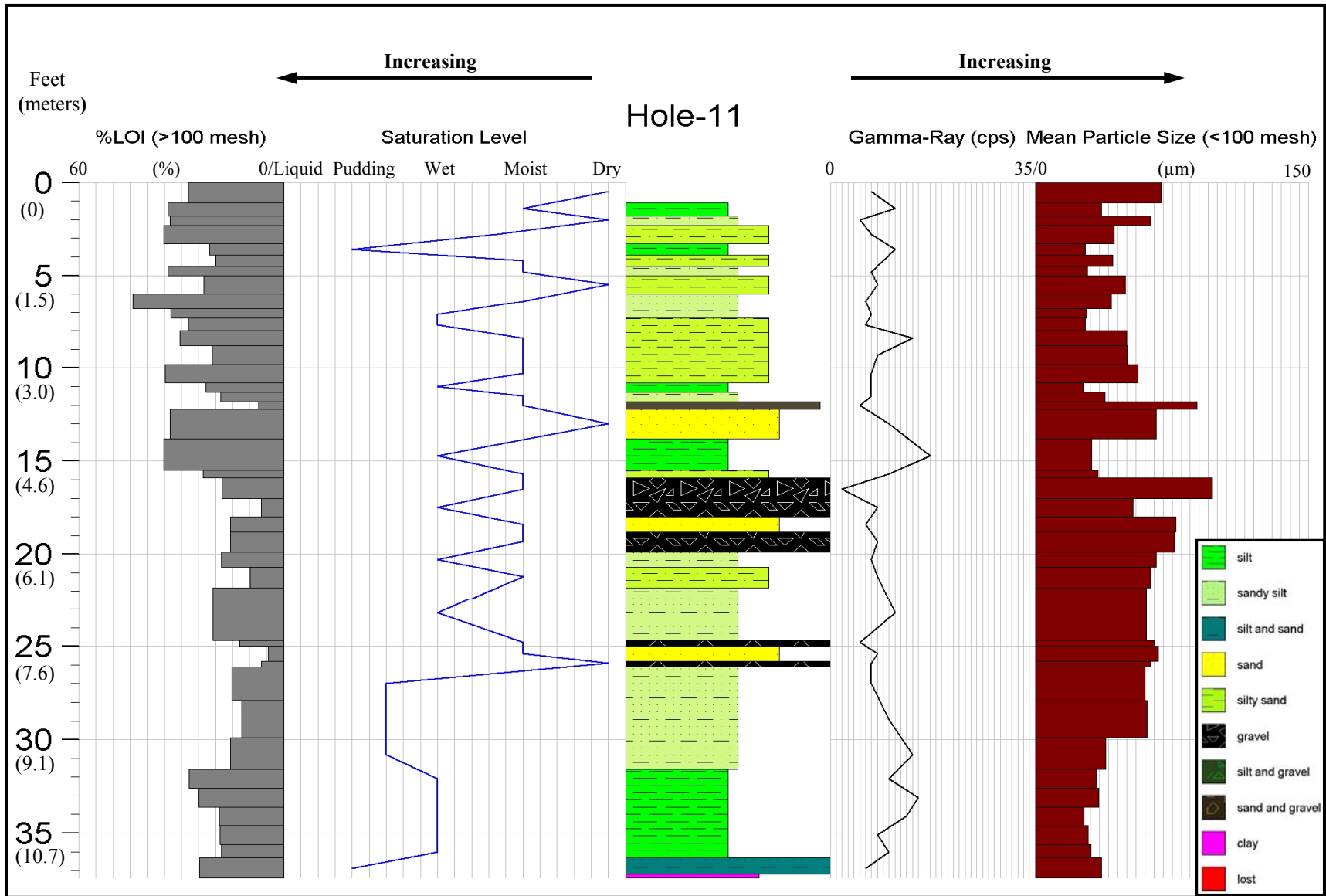
- ACAA, 2003, Fly ash facts for highway engineers: American Coal Ash Association FHWA-IF-03-019, 4th ed., June, 2003, 73 p.
- ASTM, 2000, Annual book of ASTM standards: Concrete and aggregates. Philadelphia, PA: American Society for Testing and Materials, v. 4.02, 293 p.
- Hemmings, B., and Sheetz, C., 1987, Speciation in size and density fractionated fly ash. Characterization of a low-calcium, high-iron fly ash, Materials Research Society Symposia Proceedings, Fly Ash and Coal Conversion By-Products: Characterization, Utilization and Disposal, v. 86. 186 p.
- Lanesky, D. E., Logan B, B. W., Brown, R. G., and Hine, A. C., 1979, A new approach to portable vibracoring underwater and on land: Journal of Sedimentary Petrology, v. 49, p. 654-657.
- Smith, D. G., 1992, Vibracoring: Recent innovations: Journal of Paleolimnology, v. 7, p. 137-143.
- Smith, D. G., 1998, Vibracoring: a new method for coring deep lakes: Palaeogeography, Palaeoclimatology, Palaeoecology, v. 140, p. 433-440.
- Thomas, T. A., Miller C. S., Doss, P. K., Thompson, L. D. P., and Baedke, S. J., 1991, Land-based vibracoring and vibracore analysis: Tips, tricks, and traps: Indiana Geological Survey Occasional Paper 58, 13 p.
- Vassilev, S.V., and Vassileva, C.G., 1996, Mineralogy of combustion wastes from coal-fired power stations: Fuel Processing Technology, v. 47, p. 261-280.

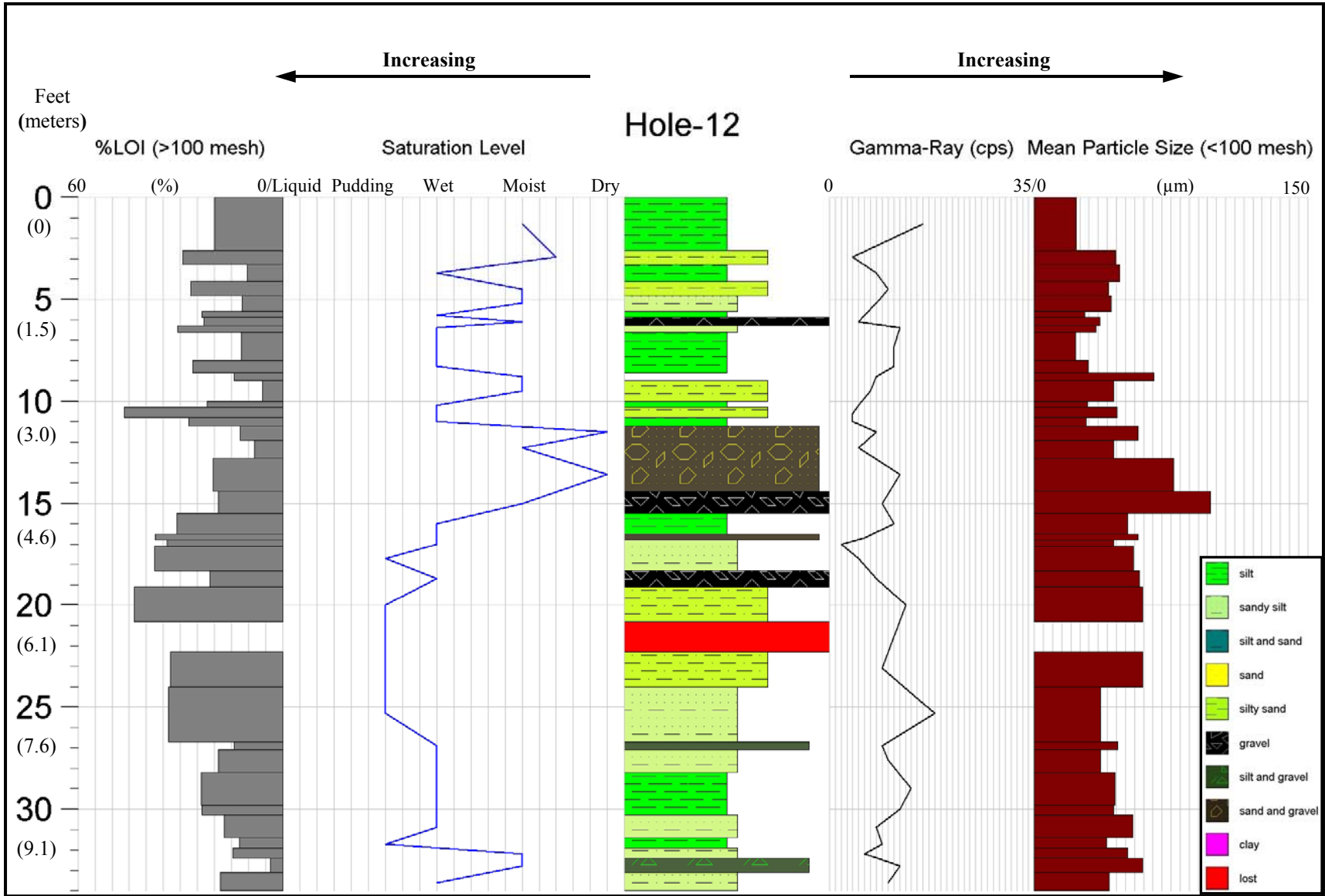
APPENDICES

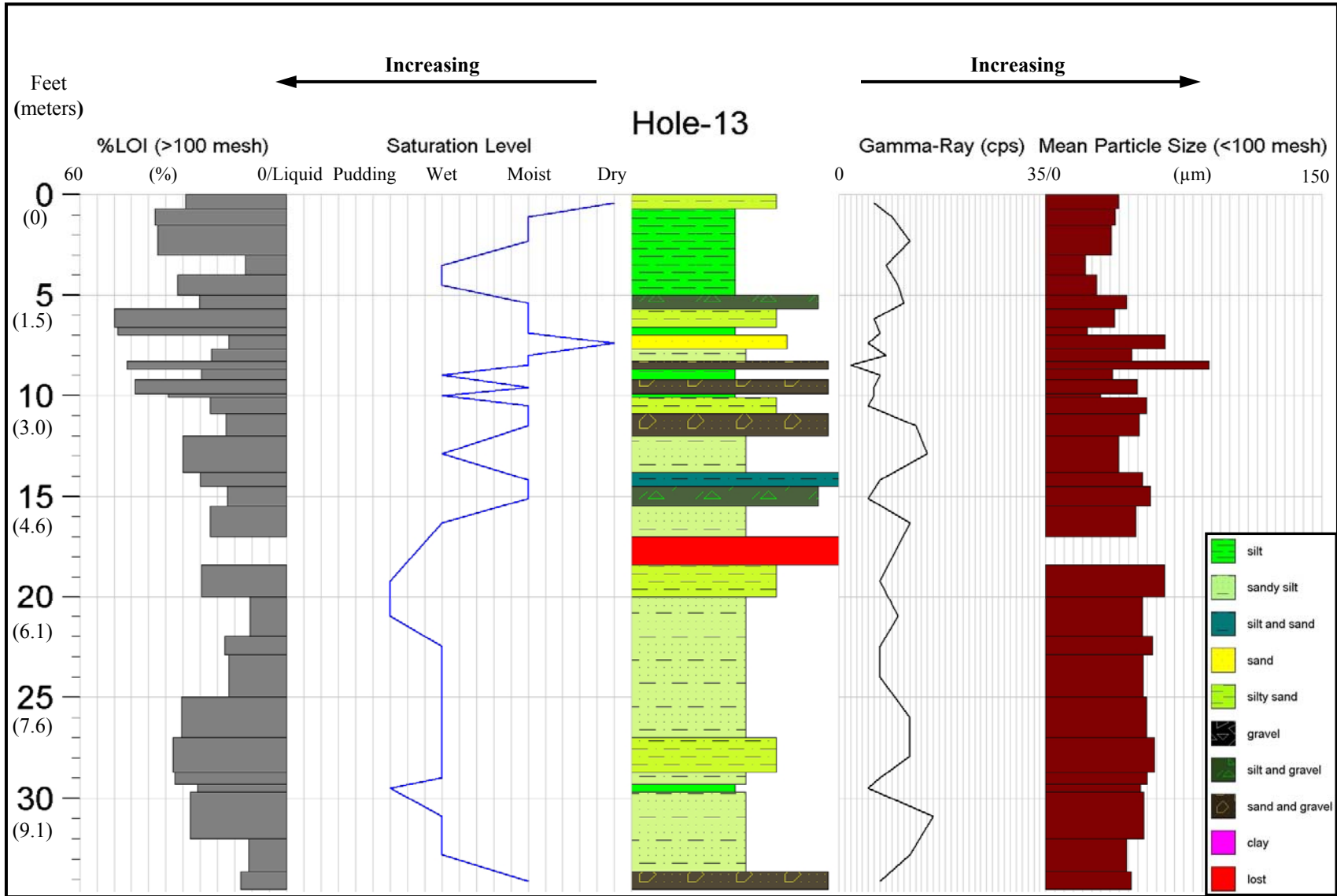
Appendix A: Sedimentologic Columns

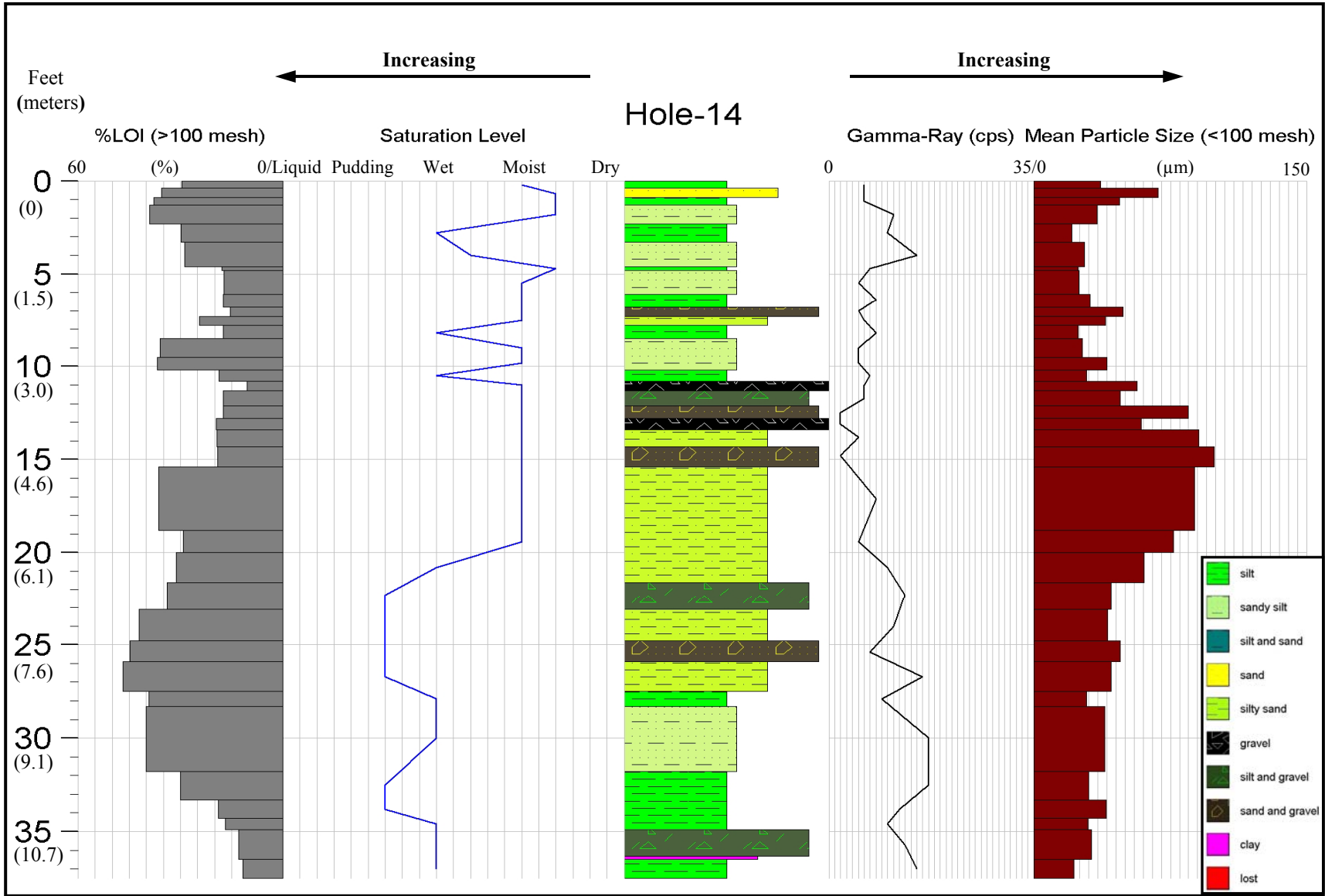


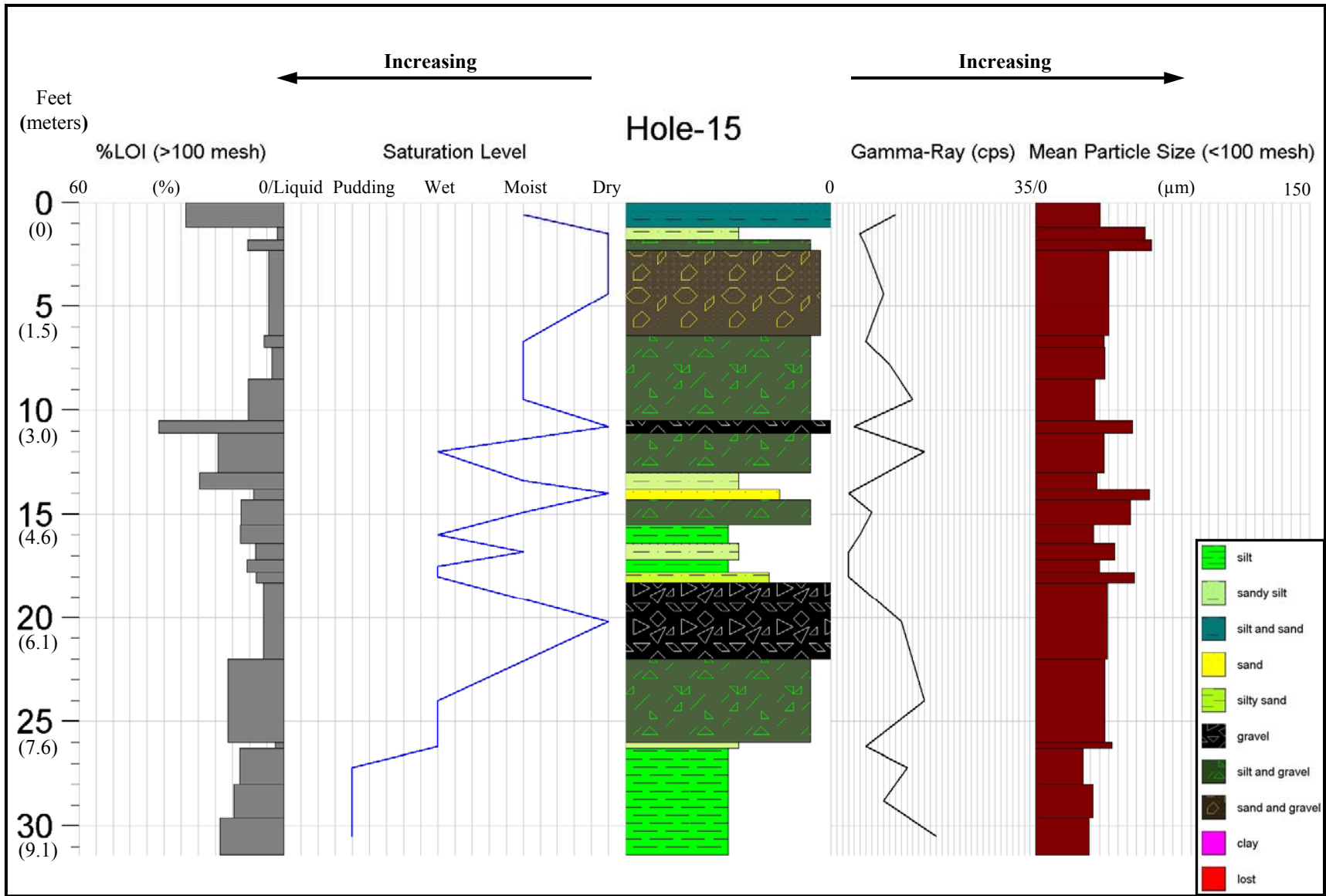


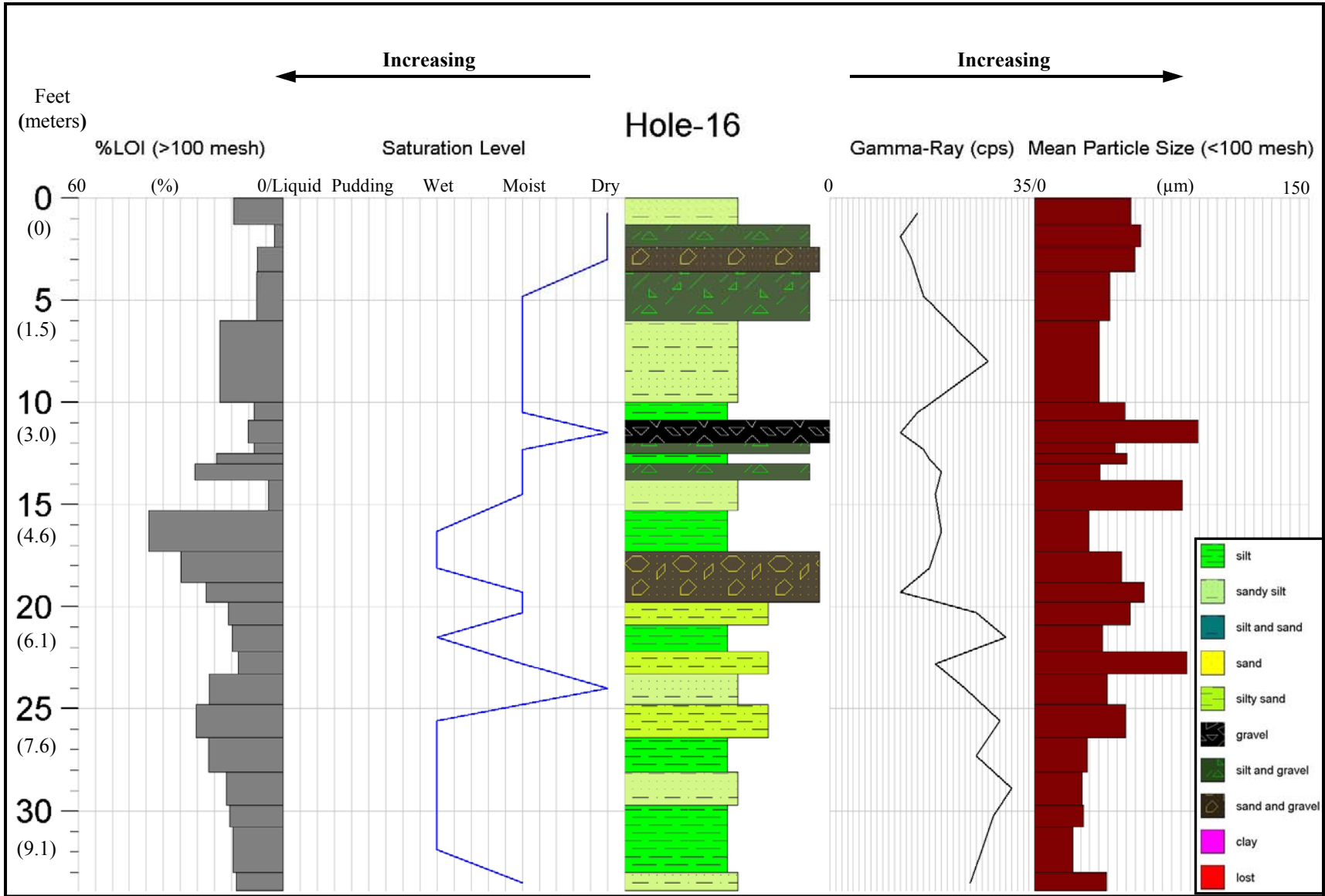


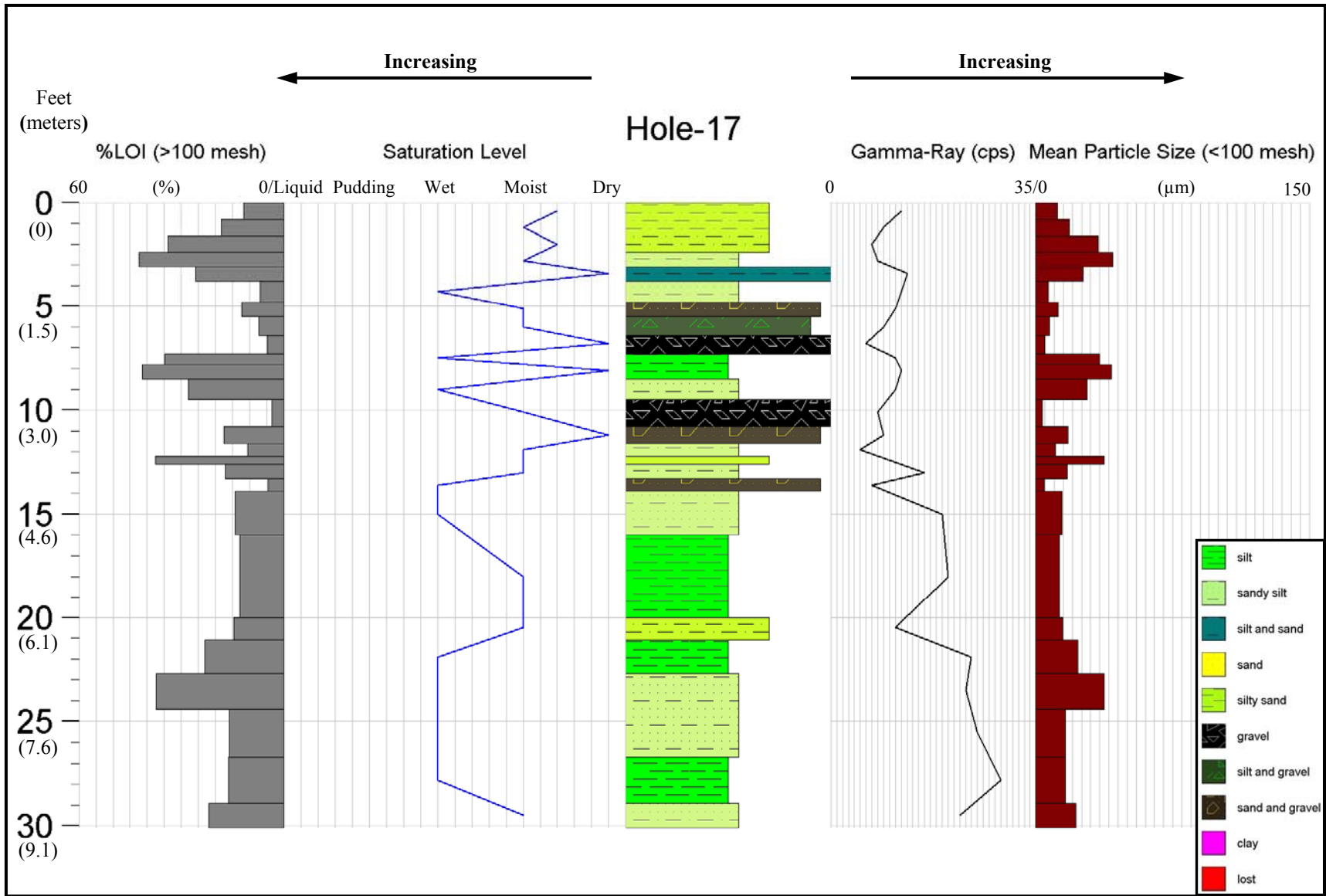


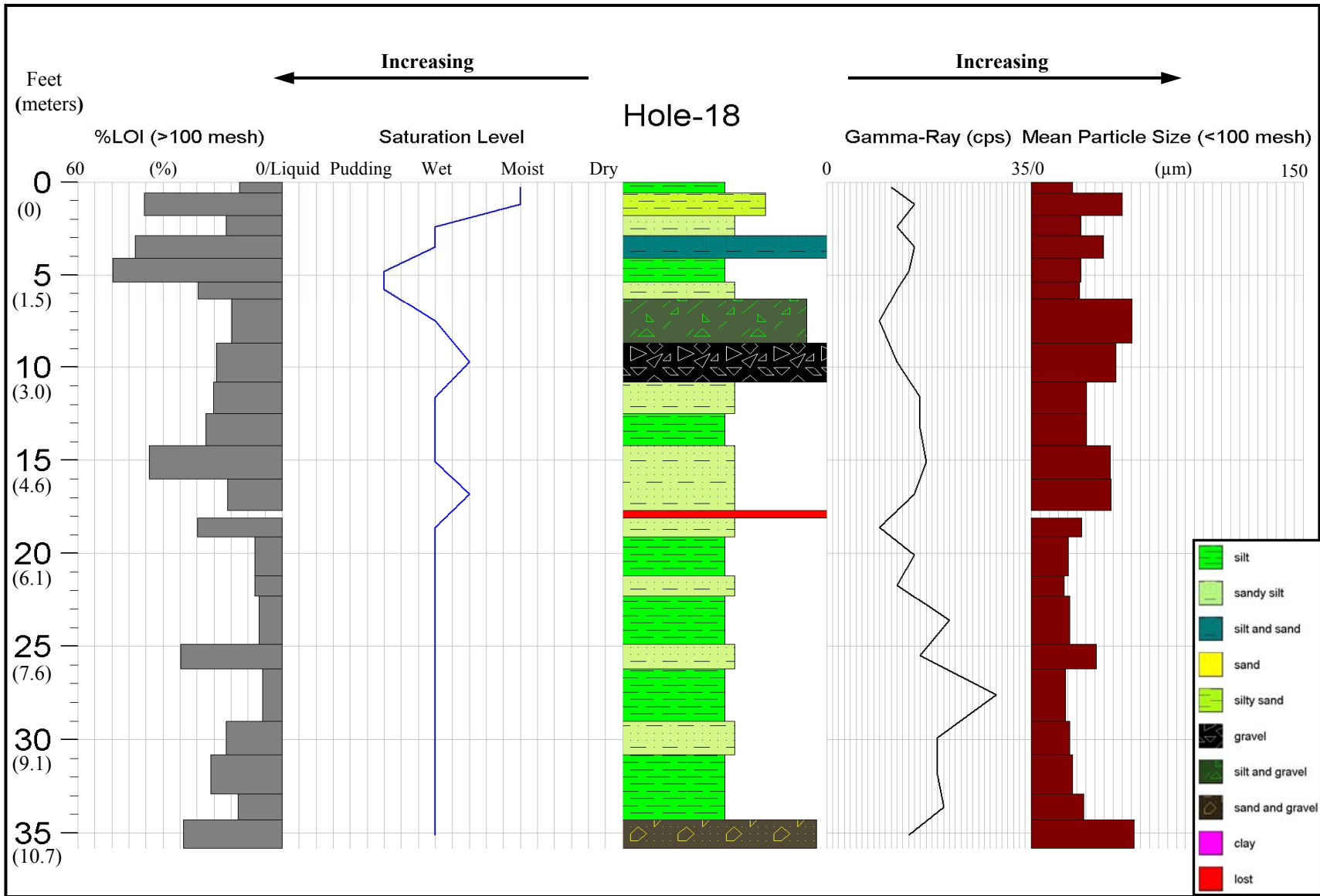


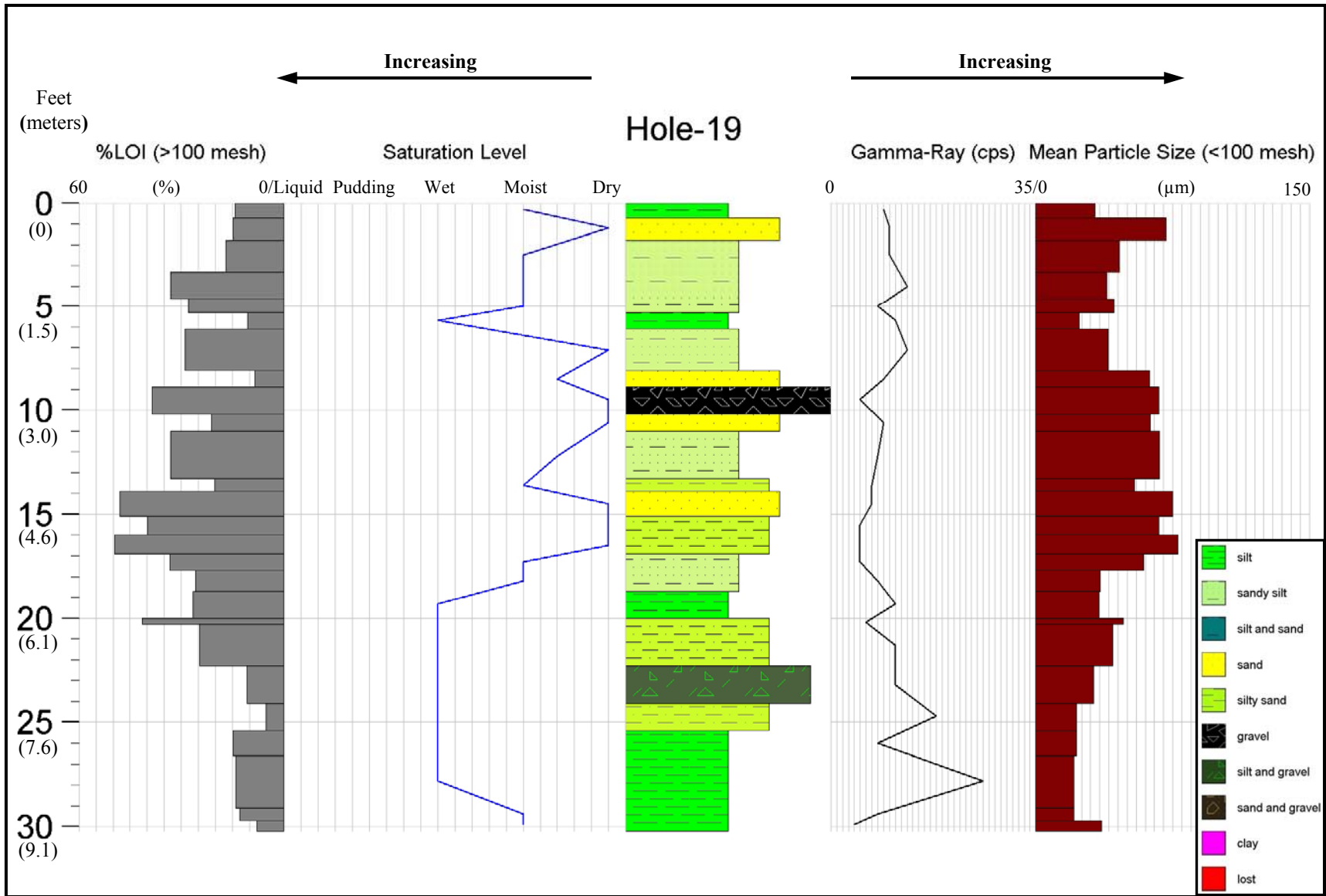


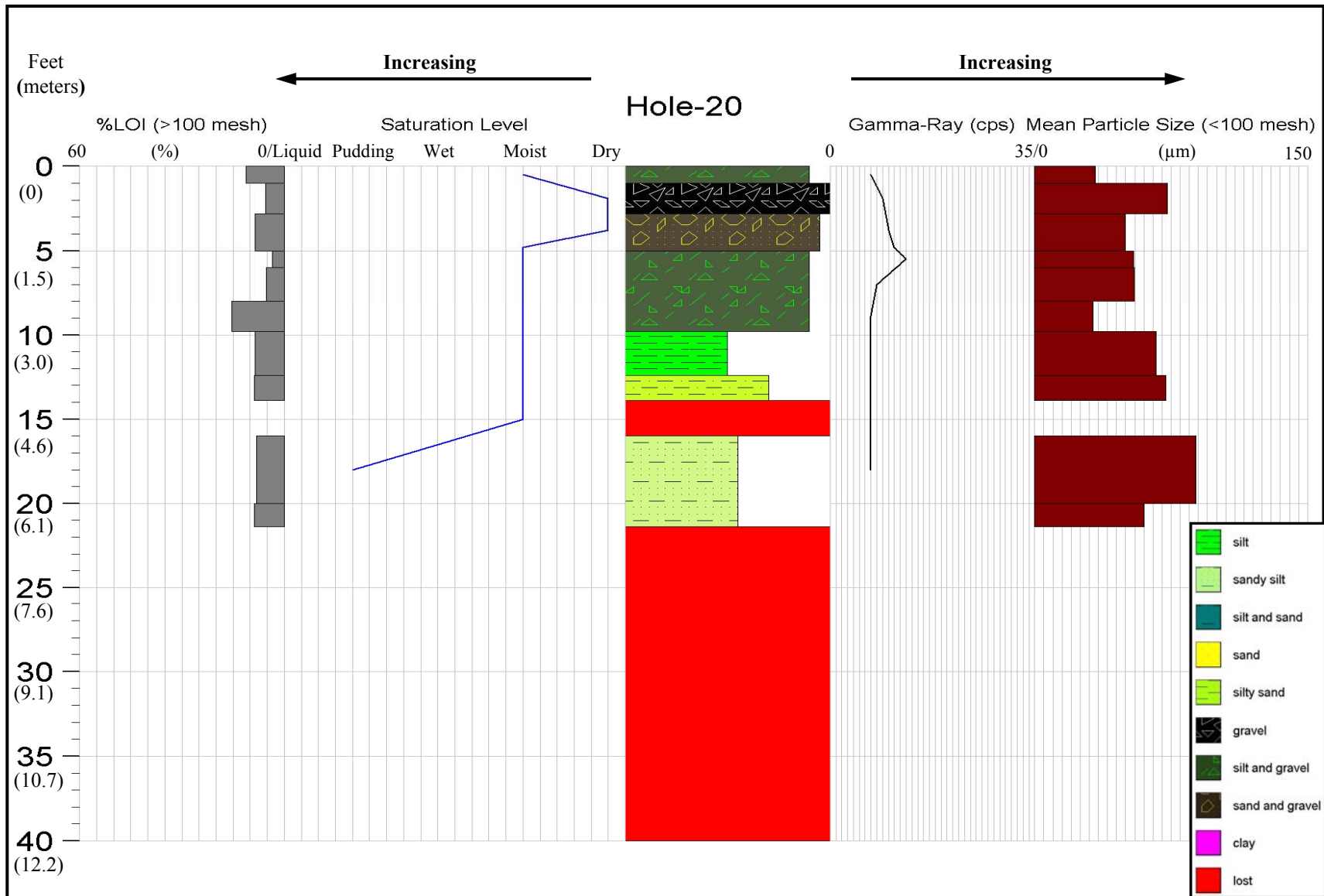












Appendix B: Vibracore Analysis Data

Hole #	Avg Depth (feet)	Avg Depth (meters)	Weight (g)		Weight %		Mean (μm)	Gamma-Ray (cps)	% LOI		Saturation Level	<5 μm %	<10 μm %
			<100	>100	<100	>100			<100	>100			
VH-8	0.2	0.05	113.5	16.7	87.2	12.8	40.0	8	1.7	27.0	moist	12.4	20.3
VH-8	0.8	0.25	424.4	20.7	95.3	4.7	28.0	6	3.9	27.1	pudding	18.7	29.4
VH-8	2.0	0.61	802.3	6.9	99.1	0.9	14.0	7	2.9	22.1	pudding	26.1	41.6
VH-8	2.9	0.88	234.0	9.5	96.1	3.9	16.0	8	3.0	15.3	wet	23.2	37.9
VH-8	3.5	1.05	341.7	161.9	67.9	32.1	34.0	9	3.6	20.4	moist	15.9	24.6
VH-8	4.8	1.47	1074.7	47.9	95.7	4.3	22.0	8	3.8	39.6	wet	22.3	33.8
VH-8	6.1	1.87	344.5	4.0	98.9	1.1	13.0	9	3.7	37.3	wet	28.4	43.8
VH-8	6.6	2.01	157.4	25.4	86.1	13.9	18.0	6	3.6	48.7	moist	24.6	37.1
VH-8	7.7	2.35	1125.4	8.6	99.2	0.8	17.0	9	2.8	21.9	pudding	25.3	38.4
VH-8	9.7	2.95	974.1	8.6	99.1	0.9	19.0	9	4.9	28.5	pudding	22.6	35.3
VH-8	10.8	3.30	215.9	4.0	98.2	1.8	16.0	10	2.8	29.5	pudding	24.9	39.0

Hole #	Avg Depth (feet)	Avg Depth (meters)	Weight (g)		Weight %		Mean (μ m)	Gamma- Ray (cps)	% LOI		Saturation Level	<5 μ m %	<10 μ m %
			<100	>100	<100	>100			<100	>100			
VH-9	0.1	0.04	164	3	98.3	1.7	35.44	7	3.2	39.4	moist	18.6	32.8
VH-9	0.5	0.17	364	1	99.7	0.3	21.09	6	2.7	18.3	moist	21.0	38.4
VH-9	0.9	0.27	100	1	98.7	1.3	36.96	8	4.8	36.2	moist	15.0	26.8
VH-9	1.2	0.36	283	1	99.6	0.4	24.36	8	1.7	16.1	moist	25.3	40.6
VH-9	2.0	0.62	343	8	97.7	2.3	52.31	4	5.3	41.0	dry	15.7	25.2
VH-9	2.7	0.83	80	2	97.6	2.4	35.66	1	5.1	37.4	moist	22.6	36.0
VH-9	2.9	0.88	68	10	86.9	13.1	Missing	Missing	4.0	53.0	dry	Missing	Missing
VH-9	3.0	0.93	85	1	98.8	1.2	22.52	3	2.3	23.2	moist	27.5	43.7
VH-9	3.3	0.99	179	4	97.8	2.2	42.46	0	6.0	51.4	moist	19.2	29.8
VH-9	3.6	1.10	226	4	98.3	1.7	30.95	3	3.5	36.8	moist	23.8	38.4
VH-9	3.9	1.20	189	2	99.0	1.0	57.83	7	4.4	46.1	moist/dry	9.8	17.4
VH-9	4.2	1.29	90	15	85.6	14.4	24.81	3	2.8	36.2	wet	26.3	42.0
VH-9	4.6	1.39	249	11	95.8	4.2	36.21	2	2.2	12.8	moist	20.9	33.4
VH-9	4.9	1.49	153	4	97.5	2.5	36.05	0	3.7	37.7	moist	19.9	32.1
VH-9	5.3	1.62	351	23	93.9	6.1	46.19	8	3.0	31.3	moist	17.5	27.2
VH-9	5.9	1.80	371	4	98.9	1.1	29.20	8	3.0	23.6	moist	24.6	38.9
VH-9	6.3	1.91	168	10	94.4	5.6	46.37	0	3.8	35.3	wet	16.1	26.1
VH-9	6.7	2.04	374	11	97.1	2.9	34.38	7	4.5	43.0	wet	23.6	37.4
VH-9	7.5	2.29	681	18	97.4	2.6	29.82	6	3.2	35.4	wet/pudding	24.9	39.4
VH-9	8.6	2.62	646	28	95.8	4.2	35.20	5	3.2	28.1	wet	22.6	35.4
VH-9	9.4	2.86	125	24	83.9	16.1	63.08	1	3.1	36.8	moist	10.8	17.2
VH-9	10.1	3.07	896	15	98.4	1.6	34.78	6	4.7	28.8	wet	24.2	38.8
VH-9	10.8	3.29	125	8	94.0	6.0	39.09	4	3.9	25.2	wet	21.7	34.0
VH-9	11.3	3.43	420	219	65.7	34.3	54.14	10	3.9	11.3	moist	14.2	22.4
VH-9	11.9	3.62	448	80	84.8	15.2	53.07	5	3.5	23.7	moist	14.0	22.0
VH-9	13.1	4.00	188	146	56.3	43.7	80.35	3	4.4	33.8	moist/dry	7.6	12.3
VH-9	14.3	4.34	135	192	41.3	58.7	53.13	2	4.7	10.0	wet	15.8	25.3
VH-9	15.0	4.57	425	13	97.0	3.0	34.70	10	4.3	23.9	wet	20.8	33.8

VH-9	16.0	4.88	608	39	94.0	6.0	57.97	7	3.9	28.0	wet/pudding	10.5	17.3
VH-9	16.8	5.11	176	62	73.9	26.1	76.94	2	4.3	30.6	wet	8.1	13.1
VH-9	17.3	5.28	336	47	87.7	12.3	68.52	8	4.0	33.9	wet	10.4	16.6
VH-9	18.4	5.60	558	125	81.7	18.3	72.98	6	3.2	33.9	wet	8.6	13.2
VH-9	19.2	5.85	104	5	95.4	4.6	68.70	1	8.2	44.7	wet/pudding	11.4	17.5
VH-9	19.7	5.99	279	3	98.9	1.1	41.40	6	5.9	21.7	pudding	19.5	29.9
VH-9	20.4	6.21	369	45	89.1	10.9	52.05	5	5.1	26.8	wet	14.1	22.6
VH-9	21.2	6.46	534	45	92.2	7.8	47.61	3	5.4	21.9	wet/pudding	15.1	24.7
VH-9	22.5	6.85	874	17	98.1	1.9	32.37	8	3.7	29.8	pudding	23.1	37.1
VH-9	23.6	7.19	360	6	98.4	1.6	27.69	4	3.1	34.1	pudding	23.3	39.0
VH-9	24.3	7.40	466	7	98.5	1.5	22.40	4	3.1	15.0	wet	26.9	44.9
VH-9	25.1	7.66	605	8	98.7	1.3	17.62	12	2.3	24.3	wet	31.7	51.3
VH-9	26.0	7.93	390	38	91.1	8.9	47.63	8	4.2	56.6	moist	16.0	25.5
VH-9	27.1	8.27	820	9	98.9	1.1	34.58	14	2.0	49.8	moist	18.2	29.2
VH-9	28.5	8.69	962	3	99.7	0.3	22.85	22	3.1	14.3	wet/pudding	23.7	39.9
VH-9	30.1	9.17	1038	3	99.7	0.3	25.79	22	2.4	17.1	pudding	23.3	37.7

Hole #	Avg Depth (feet)	Avg Depth (meters)	Weight (g)		Weight %		Mean (μ m)	Gamma- Ray (cps)	% LOI		Saturation Level	<5 μ m %	<10 μ m %
			<100	>100	<100	>100			<100	>100			
VH-10	0.5	0.14	566	11	98.1	1.9	25.68	8	3.2	38.8	moist	26.1	41.4
VH-10	1.3	0.39	475	1	99.8	0.2	23.08	8	2.9	12.7	wet	26.8	43.1
VH-10	1.9	0.57	259	35	88.1	11.9	46.01	2	2.8	28.1	moist/dry	18.9	30.0
VH-10	2.3	0.70	104	112	48.1	51.9	42.25	2	2.7	8.4	wet	20.3	31.7
VH-10	3.0	0.93	554	5	99.1	0.9	27.03	6	2.7	29.7	wet	24.7	39.4
VH-10	3.9	1.19	385	3	99.2	0.8	29.57	6	3.1	33.0	wet	26.0	40.6
VH-10	4.8	1.46	186	14	93.0	7.0	63.82	3	1.3	15.6	dry	8.1	12.1
VH-10	5.5	1.69	164	7	95.9	4.1	43.73	2	3.0	48.9	moist	17.9	27.7
VH-10	6.0	1.83	293	17	94.5	5.5	32.71	5	3.8	20.0	moist	22.7	36.2
VH-10	6.5	1.97	203	23	89.8	10.2	40.03	4	6.0	42.0	moist	23.9	37.2
VH-10	6.8	2.08	165	19	89.7	10.3	54.51	3	1.6	23.3	moist	8.9	13.5
VH-10	7.5	2.29	516	21	96.1	3.9	33.17	6	3.9	14.7	moist	23.8	37.7
VH-10	8.3	2.51	314	5	98.4	1.6	27.72	5	3.2	18.2	wet	22.8	37.6
VH-10	8.9	2.71	412	51	89.0	11.0	52.70	5	4.0	26.5	moist	13.2	21.1
VH-10	9.8	2.97	515	20	96.3	3.7	23.33	6	3.5	50.2	wet	23.5	40.3
VH-10	10.5	3.20	258	18	93.5	6.5	34.27	4	3.1	16.5	moist	21.7	35.0
VH-10	10.9	3.31	61	43	58.7	41.3	68.53	10	2.2	6.0	moist	7.0	11.5
VH-10	11.2	3.42	252	44	85.1	14.9	43.55	5	2.3	10.2	moist	17.8	28.5
VH-10	11.7	3.57	143	123	53.8	46.2	64.07	3	3.2	14.4	moist	13.9	21.6
VH-10	12.4	3.77	321	84	79.3	20.7	48.92	2	0.0	31.4	moist	19.1	29.0
VH-10	13.1	4.00	206	45	82.1	17.9	65.34	10	3.8	26.3	wet	9.8	15.3
VH-10	13.8	4.19	227	49	82.2	17.8	37.25	4	3.6	13.7	pudding	20.9	33.8
VH-10	14.4	4.38	321	91	77.9	22.1	62.24	6	4.2	23.6	wet	11.9	18.7
VH-10	14.9	4.55	143	37	79.4	20.6	66.88	2	5.0	30.7	wet	11.1	17.0
VH-10	15.5	4.74	501	38	92.9	7.1	49.17	10	4.0	27.7	wet	15.1	24.2
VH-10	16.5	5.03	loss	loss	loss	loss	loss	loss	loss	loss	loss	loss	loss
VH-10	17.3	5.28	198	6	97.1	2.9	47.24	3	10.1	27.1	wet	14.6	24.5
VH-10	18.2	5.54	323	15	95.6	4.4	53.18	8	8.6	56.5	wet	13.1	21.7

VH-10	19.2	5.84	479	24	95.2	4.8	46.03	9	6.7	50.2	wet	15.0	25.4
VH-10	20.3	6.17	605	29	95.4	4.6	47.59	7	6.3	40.5	wet	19.9	23.4
VH-10	21.3	6.50	479	14	97.2	2.8	47.42	8	7.3	44.9	wet	10.7	20.5
VH-10	22.3	6.78	405	1	99.8	0.2	46.07	5	7.8	33.9	wet	10.5	20.5
VH-10	23.0	7.01	301	3	99.0	1.0	37.71	6	5.9	46.7	wet	11.9	23.9
VH-10	23.8	7.24	315	5	98.4	1.6	37.60	7	6.5	39.2	wet	11.6	23.4
VH-10	24.5	7.45	247	2	99.2	0.8	37.60	7	4.4	28.1	wet	13.8	27.7
VH-10	25.1	7.66	302	40	88.3	11.7	43.44	5	6.0	39.3	wet	11.0	22.7
VH-10	26.0	7.92	449	39	92.0	8.0	44.00	5	7.2	39.9	wet	11.4	23.1
VH-10	26.8	8.17	234	37	86.3	13.7	51.69	5	7.7	38.0	wet	9.7	19.0
VH-10	27.5	8.39	386	34	91.9	8.1	40.92	11	5.1	37.0	wet	13.3	25.9
VH-10	28.4	8.66	331	45	88.0	12.0	46.38	11	8.5	42.6	wet	11.6	22.4
VH-10	29.3	8.94	510	9	98.3	1.7	30.53	17	3.8	22.6	wet	16.4	32.0
VH-10	30.4	9.27	538	35	93.9	6.1	40.35	10	5.0	34.9	moist	12.4	24.3
VH-10	31.5	9.61	424	4	99.1	0.9	31.96	14	3.9	12.1	wet	13.9	27.3
VH-10	32.7	9.96	447	6	98.7	1.3	37.63	11	3.2	14.4	wet	13.0	24.9
VH-10	33.8	10.30	433	11	97.5	2.5	43.00	14	2.9	15.7	wet	13.0	24.1
VH-10	34.8	10.62	409	12	97.1	2.9	50.74	7	4.0	19.2	wet	8.5	16.8
VH-10	35.7	10.88	660	3	99.5	0.5	22.40	13	2.6	36.0	wet	23.3	42.8
VH-10	36.5	11.14	251	6	97.7	2.3	33.83	13	3.1	43.3	moist	12.5	25.3

Hole #	Avg Depth (feet)	Avg Depth (meters)	Weight (g)		Weight %		Mean (μ m)	Gamma- Ray (cps)	% LOI		Saturation Level	<5 μ m %	<10 μ m %
			<100	>100	<100	>100			<100	>100			
VH-11	0.5	0.17	348	94	78.7	21.3	69.15	7	2.4	28.0	dry	4.8	8.3
VH-11	1.4	0.43	357	5	98.6	1.4	36.44	11	3.8	33.8	moist	16.7	29.9
VH-11	2.0	0.61	156	5	96.9	3.1	63.30	5	2.4	33.3	dry	5.2	8.5
VH-11	2.8	0.85	455	16	96.6	3.4	43.31	7	3.5	35.1	moist/dry	15.4	27.0
VH-11	3.6	1.10	345	2	99.4	0.6	27.32	11	3.6	21.8	pudding	20.4	36.0
VH-11	4.2	1.28	263	12	95.6	4.4	42.47	9	3.7	20.0	moist	13.8	24.6
VH-11	4.8	1.45	297	8	97.4	2.6	28.44	7	4.2	33.9	moist	22.4	39.6
VH-11	5.5	1.68	447	17	96.3	3.7	49.32	8	2.5	23.4	dry	14.6	25.2
VH-11	6.4	1.96	275	49	84.9	15.1	41.54	6	4.6	44.2	moist	15.6	28.0
VH-11	7.1	2.16	294	4	98.7	1.3	28.01	7	3.1	33.1	wet	19.6	36.2
VH-11	7.7	2.34	413	3	99.3	0.7	27.40	6	3.1	28.0	wet	21.1	37.4
VH-11	8.4	2.57	496	50	90.8	9.2	50.05	14	3.9	30.3	moist	11.5	20.7
VH-11	9.3	2.83	519	37	93.3	6.7	50.70	8	2.8	21.0	moist	10.7	19.8
VH-11	10.3	3.14	506	43	92.2	7.8	56.20	7	5.2	34.7	moist	8.7	16.0
VH-11	11.0	3.37	296	1	99.7	0.3	26.25	7	3.8	22.8	wet	15.9	31.1
VH-11	11.5	3.51	293	7	97.7	2.3	38.27	7	3.3	18.4	moist	15.6	27.9
VH-11	12.0	3.64	136	92	59.6	40.4	88.81	5	2.0	7.3	moist	4.9	8.3
VH-11	13.0	3.96	416	139	75.0	25.0	66.19	10	6.6	33.3	dry	6.3	11.7
VH-11	14.7	4.47	768	5	99.4	0.6	31.01	17	4.2	35.2	wet	14.6	29.0
VH-11	15.7	4.79	219	3	98.6	1.4	34.50	10	4.1	23.7	moist	13.2	26.0
VH-11	16.5	5.02	161	306	34.5	65.5	97.19	2	2.9	18.0	moist	2.9	5.5
VH-11	17.5	5.33	331	189	63.7	36.3	53.70	8	4.0	6.6	wet	10.2	19.2
VH-11	18.4	5.60	169	172	49.6	50.4	77.20	6	5.3	15.6	moist	5.7	10.7
VH-11	19.3	5.89	225	321	41.2	58.8	76.51	8	4.6	15.7	moist	5.5	10.4
VH-11	20.3	6.18	266	87	75.4	24.6	66.47	7	6.7	18.2	wet	5.1	9.9
VH-11	21.2	6.46	493	64	88.5	11.5	63.27	8	3.6	9.9	moist	5.2	10.0
VH-11	23.2	7.07	938	122	88.5	11.5	61.07	11	3.8	20.7	wet	5.0	9.8
VH-11	24.8	7.57	129	57	69.4	30.6	65.06	5	3.9	13.0	moist	5.0	9.9

VH-11	25.4	7.73	256	89	74.2	25.8	67.44	8	2.6	4.5	moist	3.9	7.5
VH-11	25.9	7.90	109	38	74.1	25.9	63.06	7	3.7	6.6	dry	4.5	9.2
VH-11	27.0	8.23	533	99	84.3	15.7	60.34	7	4.5	15.1	wet/pudding	4.7	9.7
VH-11	28.9	8.81	634	69	90.2	9.8	61.17	10	4.4	12.4	wet/pudding	5.1	10.4
VH-11	30.8	9.37	779	23	97.1	2.9	38.49	14	3.3	15.7	wet/pudding	13.7	25.8
VH-11	32.1	9.78	567	5	99.1	0.9	33.55	10	3.1	27.8	wet	12.5	24.4
VH-11	33.1	10.08	466	10	97.9	2.1	34.62	15	2.6	24.9	wet	12.9	25.0
VH-11	34.1	10.39	438	3	99.3	0.7	26.66	13	2.3	18.8	wet	14.6	28.7
VH-11	35.1	10.69	340	1	99.7	0.3	28.97	8	2.7	18.7	wet	13.3	26.5
VH-11	36.0	10.96	140	1	99.3	0.7	30.61	10	3.4	18.3	wet	12.9	25.7
VH-11	36.9	11.24	81	3	96.4	3.6	36.37	6	3.4	24.7	pudding	13.5	26.4

Hole #	Avg Depth (feet)	Avg Depth (meters)	Weight (g)		Weight %		Mean (μ m)	Gamma- Ray (cps)	% LOI		Saturation Level	<5 μ m %	<10 μ m %
			<100	>100	<100	>100			<100	>100			
VH-12	1.3	0.39	1566	7	99.6	0.4	22.95	16	5.9	20.0	moist	22.1	40.5
VH-12	2.9	0.89	441	16	96.5	3.5	44.57	4	3.6	29.3	moist/dry	14.4	25.7
VH-12	3.7	1.12	400	53	88.3	11.7	46.87	8	3.4	10.5	wet	12.2	22.8
VH-12	4.5	1.36	497	18	96.5	3.5	40.51	10	3.6	26.9	moist	15.3	26.9
VH-12	5.2	1.59	485	14	97.2	2.8	42.09	8	2.1	11.9	moist	14.2	25.5
VH-12	5.8	1.75	190	2	99.0	1.0	27.65	6	2.8	23.8	wet	19.4	36.0
VH-12	6.1	1.85	188	43	81.4	18.6	35.86	5	3.0	23.1	moist	18.2	32.8
VH-12	6.4	1.96	228	2	99.1	0.9	33.98	12	3.6	30.8	wet	19.1	33.3
VH-12	7.3	2.22	812	3	99.6	0.4	22.72	11	2.9	12.2	wet	23.3	41.8
VH-12	8.3	2.53	432	3	99.3	0.7	29.66	11	2.9	26.5	wet	19.6	34.6
VH-12	8.8	2.68	240	20	92.3	7.7	65.61	8	1.7	14.3	moist	5.9	10.8
VH-12	9.5	2.90	568	78	87.9	12.1	43.71	7	2.5	5.9	moist	12.9	23.4
VH-12	10.2	3.10	215	1	99.5	0.5	29.15	5	3.0	22.1	wet	14.3	28.4
VH-12	10.6	3.23	256	7	97.3	2.7	45.47	4	5.2	46.5	wet	11.0	21.6
VH-12	11.0	3.35	202	1	99.5	0.5	28.45	4	3.4	27.5	wet	14.9	29.2
VH-12	11.5	3.52	284	61	82.3	17.7	56.98	8	3.0	12.5	dry	8.0	15.5
VH-12	12.3	3.76	356	112	76.1	23.9	43.57	5	3.0	8.3	moist	14.7	27.2
VH-12	13.6	4.14	402	267	60.1	39.9	76.51	12	3.7	20.5	dry	4.8	9.0
VH-12	15.0	4.56	207	285	42.1	57.9	96.49	9	3.5	18.9	moist	4.1	7.8
VH-12	16.0	4.88	503	45	91.8	8.2	51.04	11	4.0	31.0	wet	10.2	19.9
VH-12	16.7	5.08	111	41	73.0	27.0	56.86	6	3.5	37.4	wet	9.6	18.8
VH-12	17.0	5.17	120	4	96.8	3.2	43.62	2	4.7	33.9	wet	12.9	25.2
VH-12	17.7	5.40	408	54	88.3	11.7	54.28	5	7.1	37.5	wet/pudding	9.5	18.1
VH-12	18.7	5.70	255	125	67.1	32.9	57.72	8	7.9	21.4	wet	8.4	16.6
VH-12	20.0	6.08	510	181	73.8	26.2	59.54	13	7.9	43.6	wet/pudding	7.9	15.5
VH-12	21.5	6.57	loss	loss	loss	loss	loss	loss	loss	loss	loss	loss	loss
VH-12	23.1	7.05	639	258	71.2	28.8	59.63	9	6.4	32.9	wet/pudding	7.5	14.8
VH-12	25.3	7.72	1794	31	98.3	1.7	36.49	18	6.9	33.5	wet/pudding	12.9	25.4

VH-12	26.9	8.19	201	33	85.9	14.1	45.64	9	4.7	14.3	wet	11.7	23.1
VH-12	27.6	8.42	570	30	95.0	5.0	36.46	10	4.2	18.9	wet	13.0	25.9
VH-12	29.0	8.83	892	34	96.3	3.7	44.11	14	6.0	23.9	wet	12.7	23.1
VH-12	30.0	9.16	287	14	95.3	4.7	43.58	12	5.3	23.8	wet	11.3	22.3
VH-12	30.9	9.41	542	46	92.2	7.8	54.09	8	4.6	17.2	wet	7.4	14.4
VH-12	31.7	9.65	233	1	99.6	0.4	39.72	9	3.0	12.8	wet/pudding	11.2	21.5
VH-12	32.2	9.80	267	15	94.7	5.3	51.20	6	6.9	14.7	moist	7.2	14.3
VH-12	32.8	9.99	282	119	70.3	29.7	59.50	12	3.8	3.7	moist	7.2	13.8
VH-12	33.6	10.23	534	21	96.2	3.8	41.20	10	3.1	18.4	wet	11.7	22.5

Hole #	Avg Depth (feet)	Avg Depth (meters)	Weight (g)		Weight %		Mean (µm) <100	Gamma- Ray (cps)	% LOI		Saturation Level	<5 µm %	<10 µm %
			<100	>100	<100	>100			<100	>100			
VH-13	0.4	0.11	479	8	98.4	7.5	39.53	6	2.1	29.3	dry	15.3	26.5
VH-13	1.1	0.35	460	33	93.3	6.7	37.65	9	4.0	38.2	moist	17.9	31.5
VH-13	2.3	0.70	964	25	97.5	2.5	35.52	12	3.6	37.3	moist	19.3	32.3
VH-13	3.5	1.08	550	3	99.5	0.5	21.48	8	2.6	11.9	wet	26.1	45.5
VH-13	4.5	1.37	661	6	99.1	0.9	27.68	10	2.7	31.6	wet	21.3	37.5
VH-13	5.4	1.64	311	64	82.9	17.1	43.98	11	3.6	25.2	moist	13.1	24.2
VH-13	6.2	1.89	485	43	91.9	8.1	37.36	6	6.0	49.9	moist	17.7	31.5
VH-13	6.9	2.10	272	4	98.6	1.4	22.65	7	3.5	48.9	moist	25.6	45
VH-13	7.4	2.26	246	41	85.7	14.3	64.75	5	2.4	16.8	dry	6.72	12.4
VH-13	8.0	2.45	360	22	94.2	5.8	46.65	8	3.1	21.7	moist	13	23.3
VH-13	8.5	2.60	67	40	62.6	37.4	88.71	2	7.8	46.2	moist	4.36	8.43
VH-13	9.0	2.74	272	15	94.8	5.2	36.28	7	3.3	24.6	wet	17.6	31.1
VH-13	9.6	2.92	319	27	92.2	7.8	49.65	6	3.0	44.0	moist	8.89	17.1
VH-13	10.0	3.06	131	1	99.2	0.8	29.81	6	2.6	34.4	wet	14.3	28.1
VH-13	10.5	3.21	263	55	82.7	17.3	54.74	5	3.4	22.1	moist	11.7	21.3
VH-13	11.5	3.49	440	145	75.2	24.8	50.67	13	3.3	17.5	moist	12.8	23.3
VH-13	12.9	3.94	1209	71	94.5	5.5	39.42	15	3.6	30.0	wet	16.3	28.6
VH-13	14.2	4.33	264	57	82.2	17.8	52.46	7	4.7	25.0	moist	12.6	22.4
VH-13	15.1	4.60	290	138	67.8	32.2	56.75	5	3.7	17.2	moist	11.1	20
VH-13	16.3	4.97	606	95	86.4	13.6	48.97	12	3.3	22.1	wet	9.81	19.1
VH-13	17.7	5.40	loss	loss	loss	loss	loss	loss	loss	loss	loss	loss	loss
VH-13	19.2	5.85	434	110	79.8	20.2	64.41	7	6.1	24.6	wet/pudding	6.07	11.6
VH-13	21.0	6.40	565	110	83.7	16.3	52.62	10	3.1	10.6	wet/pudding	6.37	12.2
VH-13	22.5	6.85	303	15	95.3	4.7	58.10	7	3.6	17.9	wet	5.27	10.7
VH-13	24.0	7.30	744	31	96.0	4.0	52.96	7	3.6	16.8	wet	7.32	14.4
VH-13	26.0	7.92	890	36	96.1	3.9	54.65	12	3.2	30.5	wet	7.42	14.2
VH-13	27.9	8.50	826	32	96.3	3.7	59.18	12	3.7	33.0	wet	6.77	12.6
VH-13	29.0	8.85	255	14	94.8	5.2	55.00	7	3.5	32.4	wet	8.03	15.2

VH-13	29.5	9.00	200	3	98.5	1.5	51.40	5	3.1	25.8	wet/pudding	8.38	16
VH-13	30.9	9.41	1017	37	96.5	3.5	53.14	16	3.2	28.0	wet	7.46	14.3
VH-13	32.8	10.01	657	217	75.2	24.8	43.82	12	2.2	11.0	wet	7.56	15.3
VH-13	34.1	10.40	330	36	90.2	9.8	46.47	7	4.0	13.3	moist	10	19.4

Hole #	Avg Depth (feet)	Avg Depth (meters)	Weight (g)		Weight %		Mean (μ m)	Gamma- Ray (cps)	% LOI		Saturation Level	<5 μ m %	<10 μ m %
			<100	>100	<100	>100			<100	>100			
VH-14	0.2	0.06	253.4	5.3	98.0	2.0	36.63	6	3.5	29.6	moist	15.3	28.7
VH-14	0.7	0.20	176.4	27.1	86.7	13.3	68.16	6	4.1	35.5	moist/dry	6.38	11.8
VH-14	1.1	0.34	223	7	97.0	3.0	46.87	6	4.6	37.8	moist/dry	11	20.9
VH-14	1.8	0.56	608.6	4.4	99.3	0.7	34.65	11	3.3	39.1	moist/dry	14.9	27.7
VH-14	2.8	0.86	717	5	99.3	0.7	20.69	10	4.8	29.7	wet	22.7	41.9
VH-14	4.0	1.21	789	4	99.5	0.5	27.64	15	3.9	28.7	moist/wet	21.7	37.9
VH-14	4.7	1.44	145	3	98.0	2.0	24.21	7	3.8	17.9	moist/dry	19.8	37.6
VH-14	5.5	1.66	769	12	98.5	1.5	24.81	5	2.8	17.3	moist	19	36.4
VH-14	6.4	1.96	391	9	97.8	2.3	30.94	8	3.9	17.5	moist	19.3	35.2
VH-14	7.0	2.13	233	32	87.9	12.1	49.06	5	3.3	15.4	moist	10.6	20.5
VH-14	7.5	2.30	317	10	96.9	3.1	39.28	6	5.3	24.5	moist	14.5	27.5
VH-14	8.2	2.49	510	5	99.0	1.0	24.40	8	2.7	17.4	wet	22.4	41.1
VH-14	9.0	2.74	494	23	95.6	4.4	26.46	5	4.6	35.9	moist	12.1	24
VH-14	9.8	3.00	348	8	97.8	2.2	40.00	5	4.0	36.8	moist	11.5	22.5
VH-14	10.5	3.20	467	3	99.4	0.6	28.99	7	2.2	18.7	wet	14.6	29.1
VH-14	11.0	3.37	232	35	86.9	13.1	56.52	6	1.9	10.5	moist	7.59	14.4
VH-14	11.7	3.56	347	52	87.0	13.0	47.62	6	4.2	17.4	moist	12.6	24
VH-14	12.5	3.80	164	153	51.7	48.3	84.62	2	3.0	17.5	moist	3.28	6.26
VH-14	13.1	4.00	177	85	67.6	32.4	58.87	2	3.0	19.5	moist	8.85	16.9
VH-14	13.8	4.22	254	110	69.8	30.2	90.72	5	3.2	19.3	moist	2.34	4.25
VH-14	14.8	4.52	233	291	44.5	55.5	99.00	2	2.6	19.1	moist	2.75	5.19
VH-14	17.1	5.22	882	313	73.8	26.2	88.18	8	4.3	36.3	moist	3.38	6.33
VH-14	19.4	5.92	272	122	69.0	31.0	76.87	5	5.0	29.2	moist	5.05	9.67
VH-14	20.8	6.34	531	88	85.8	14.2	60.59	10	6.6	31.3	wet	7.34	14.2
VH-14	22.3	6.81	689	72	90.5	9.5	42.31	13	4.2	33.9	wet/pudding	13.7	25.7
VH-14	24.0	7.30	629	104	85.8	14.2	40.38	11	6.5	42.1	wet/pudding	8.31	16.2
VH-14	25.4	7.73	414	88	82.5	17.5	47.50	7	8.5	44.7	wet/pudding	7.41	14.2
VH-14	26.7	8.14	656	28	95.9	4.1	42.43	16	7.1	46.8	moist-wet	11.5	22.5
VH-14	27.9	8.51	363	5	98.6	1.4	28.93	9	5.5	39.2	wet	15.3	30.7

VH-14	30.0	9.16	1444	41	97.2	2.8	39.05	17	6.5	40.0	wet	12.6	24.8
VH-14	32.5	9.91	666	10	98.5	1.5	30.22	17	4.2	30.0	wet/pudding	16.5	31.3
VH-14	33.8	10.29	476	12	97.5	2.5	39.92	12	4.3	18.9	wet/pudding	13	24.2
VH-14	34.6	10.54	340	2	99.4	0.6	29.79	10	2.8	16.8	wet	15.1	29.4
VH-14	35.7	10.88	431	23	94.9	5.1	31.76	13	3.0	13.0	wet	17.4	33
VH-14	37.0	11.28	562	3	99.5	0.5	22.04	15	2.4	11.8	wet	19.8	38.2

Hole #	Avg Depth (feet)	Avg Depth (meters)	Weight (g)		Weight %		Mean (μm) <100	Gamma-Ray (cps)	% LOI		Saturation Level	<5 μm %	<10 μm %
			<100	>100	<100	>100			<100	>100			
VH-15	0.6	0.18	685	2	99.7	0.3	35.23	11	3.3	28.8	moist	18.3	32.3
VH-15	1.5	0.46	369	143	72.1	27.9	59.69	5	1.7	2.0	dry	10.2	19.3
VH-15	2.1	0.64	136	185	42.4	57.6	63.51	6	2.9	10.7	dry	8.3	15.0
VH-15	4.4	1.33	589	471	55.6	44.4	39.81	9	3.3	4.4	dry	16.1	28.9
VH-15	6.7	2.04	290	98	74.7	25.3	37.42	6	2.9	5.8	moist	16.9	29.8
VH-15	7.8	2.36	931	191	83.0	17.0	37.87	10	2.4	3.5	moist	15.2	27.6
VH-15	9.5	2.90	1387	191	87.9	12.1	32.50	14	2.8	10.5	moist	17.1	31.2
VH-15	10.8	3.29	190	98	66.0	34.0	53.00	4	1.9	36.6	dry	9.6	17.7
VH-15	12.0	3.67	1177	48	96.1	3.9	37.33	16	2.5	19.3	wet	15.4	29.1
VH-15	13.4	4.09	470	14	97.1	2.9	33.50	7	4.3	24.6	moist	15.9	30.8
VH-15	14.0	4.28	172	27	86.4	13.6	62.27	3	2.4	8.8	dry	6.0	11.4
VH-15	14.9	4.53	618	76	89.0	11.0	51.95	7	4.5	12.5	moist	11.5	22.7
VH-15	16.0	4.86	534	16	97.1	2.9	31.53	5	3.3	12.7	wet	17.3	32.8
VH-15	16.8	5.12	402	20	95.3	4.7	43.21	3	4.3	8.3	moist	12.4	24.0
VH-15	17.5	5.32	242	10	96.0	4.0	34.77	3	4.2	10.9	wet	15.4	29.1
VH-15	18.0	5.50	225	36	86.2	13.8	54.01	3	3.5	8.2	wet	9.5	18.5
VH-15	20.2	6.15	792	385	67.3	32.7	39.31	12	4.1	5.9	dry	15.0	28.1
VH-15	24.0	7.32	1601	771	67.5	32.5	37.70	16	6.0	16.3	wet	14.5	27.9
VH-15	26.2	7.98	350	116	75.1	24.9	41.77	6	5.7	2.6	wet	15.6	30.3
VH-15	27.2	8.28	1123	31	97.3	2.7	25.70	13	3.7	12.9	pudding	19.6	37.1
VH-15	28.8	8.78	717	10	98.6	1.4	31.13	9	4.3	14.6	pudding	16.2	30.8
VH-15	30.5	9.30	849	12	98.6	1.4	29.23	18	2.4	18.7	pudding	17.9	33.3

Hole #	Avg Depth (feet)	Avg Depth (meters)	Weight (g)		Weight %		Mean (μm)	Gamma-Ray (cps)	% LOI		Saturation Level	<5 μm %	<10 μm %
			<100	>100	<100	>100			<100	>100			
VH-16	0.7	0.20	680	44	93.9	6.1	52.72	15	2.0	14.4	dry	10.0	18.3
VH-16	1.9	0.57	399	297	57.3	42.7	58.16	12	2.2	2.5	dry	9.2	16.5
VH-16	3.0	0.91	549	219	71.5	28.5	54.81	14	3.1	7.5	dry	10.1	18.4
VH-16	4.8	1.46	834	92	90.1	9.9	41.18	16	3.1	7.7	moist	15.6	28.0
VH-16	8.0	2.44	2167	184	92.2	7.8	35.35	27	5.0	18.5	moist	15.9	29.6
VH-16	10.5	3.19	557	38	93.6	6.4	49.39	15	3.7	8.5	moist	17.1	30.7
VH-16	11.5	3.49	160	33	82.9	17.1	89.59	12	1.6	10.2	dry	3.5	6.3
VH-16	12.3	3.73	192	96	66.7	33.3	43.76	16	3.7	8.5	moist	14.8	27.0
VH-16	12.8	3.89	247	18	93.2	6.8	50.59	17	6.1	19.5	moist	9.8	20.4
VH-16	13.4	4.09	787	12	98.5	1.5	35.71	19	4.2	25.9	moist	14.3	27.3
VH-16	14.5	4.43	443	160	73.5	26.5	80.64	18	3.8	4.2	moist	10.3	18.9
VH-16	16.3	4.97	1134	16	98.6	1.4	29.57	19	3.7	39.4	wet	17.0	31.4
VH-16	18.1	5.51	693	67	91.2	8.8	47.42	17	4.7	29.8	wet	9.8	19.5
VH-16	19.3	5.88	358	49	88.0	12.0	59.90	12	4.1	22.6	moist	9.1	17.9
VH-16	20.3	6.20	564	51	91.7	8.3	52.29	25	3.7	16.1	moist	9.4	17.6
VH-16	21.5	6.57	631	14	97.8	2.2	36.90	30	1.7	14.8	wet	13.8	26.1
VH-16	22.8	6.93	445	9	98.0	2.0	83.45	18	3.4	13.1	moist	7.0	13.1
VH-16	24.0	7.33	548	12	97.9	2.1	39.46	23	2.4	21.6	dry	13.8	26.0
VH-16	25.6	7.80	767	27	96.6	3.4	49.85	29	2.5	25.4	wet	10.5	19.6
VH-16	27.3	8.31	795	3	99.6	0.4	28.89	25	1.9	21.7	wet	17.1	32.1
VH-16	28.9	8.80	781	4	99.5	0.5	26.05	31	1.8	16.5	wet	19.1	35.3
VH-16	30.2	9.21	923	3	99.7	0.3	26.73	28	3.1	15.6	wet	18.0	33.9
VH-16	31.9	9.72	1382	9	99.4	0.6	20.68	26	1.5	14.7	wet	21.5	41.0
VH-16	33.5	10.20	752	5	99.3	0.7	39.37	24	1.7	13.7	moist	13.6	25.3

Hole #	Avg Depth (feet)	Avg Depth (meters)	Weight (g)		Weight %		Mean (μm)	Gamma-Ray (cps)	% LOI		Saturation Level	<5 μm %	<10 μm %
			<100	>100	<100	>100			<100	>100			
VH-17	0.4	0.13	479	21	95.8	4.2	40.69	12	2.0	11.7	moist/dry	13.0	24.2
VH-17	1.2	0.37	523	6	98.9	1.1	29.21	9	3.1	18.4	moist	20.6	36.9
VH-17	2.0	0.61	459	29	94.1	5.9	48.37	7	3.1	34.0	moist/dry	15.1	27.2
VH-17	2.8	0.84	427	8	98.2	1.8	54.10	8	3.9	42.3	moist	14.1	25.1
VH-17	3.4	1.05	389	35	91.7	8.3	48.29	13	3.2	25.8	dry	12.3	21.8
VH-17	4.3	1.30	635	114	84.8	15.2	36.02	12	2.9	6.9	wet	16.8	31.1
VH-17	5.1	1.56	468	65	87.8	12.2	37.72	11	3.5	12.3	moist	15.6	28.9
VH-17	6.0	1.82	422	66	86.5	13.5	45.67	9	3.0	7.4	moist	11.6	22.0
VH-17	6.8	2.08	94	140	40.2	59.8	63.31	6	2.5	4.9	dry	8.9	16.9
VH-17	7.5	2.29	205	5	97.6	2.4	33.54	11	3.2	34.9	wet	22.2	39.7
VH-17	8.1	2.48	170	4	97.7	2.3	42.43	12	3.1	41.5	dry	10.1	19.8
VH-17	9.0	2.74	588	52	91.9	8.1	49.82	11	3.1	28	wet	12.1	21.9
VH-17	10.1	3.09	361	312	53.6	46.4	47.90	8	3.2	3.5	moist	13.3	24.0
VH-17	11.2	3.40	383	40	90.5	9.5	42.86	9	3.6	17.5	dry	12.8	24.1
VH-17	11.9	3.62	276	33	89.3	10.7	39.27	5	4.2	10.7	moist	13.7	26.1
VH-17	12.4	3.77	229	3	98.7	1.3	41.29	10	5.2	37.5	moist	14.7	26.9
VH-17	13.0	3.95	467	34	93.2	6.8	37.28	16	2.4	17.1	moist	15.4	27.8
VH-17	13.6	4.15	139	113	55.2	44.8	51.92	7	2.9	4.7	wet	12.2	22.2
VH-17	15.0	4.56	1478	45	97.0	3.0	29.59	19	4.3	14.2	wet	18.0	33.8
VH-17	18.0	5.49	1731	80	95.6	4.4	33.73	20	7.1	13	moist	13.6	27.5
VH-17	20.5	6.26	580	68	89.5	10.5	31.13	11	5.9	14.6	moist	17.8	33.4
VH-17	21.9	6.67	806	3	99.6	0.4	18.32	24	2.1	23.1	wet	26.1	45.8
VH-17	23.5	7.18	923	19	98.0	2.0	25.84	23	2.8	37.3	wet	20.5	36.3
VH-17	25.5	7.79	1081	29	97.4	2.6	27.45	25	2.4	16	wet	20.1	36.6
VH-17	27.8	8.47	1095	3	99.7	0.3	23.72	29	1.4	16.2	wet	17.5	34.9
VH-17	29.5	8.99	617	5	99.2	0.8	30.43	22	1.9	22	wet/dry	17.0	32.8

Hole #	Avg Depth (feet)	Avg Depth (meters)	Weight (g)		Weight %		Mean (µm)	Gamma-Ray (cps)	% LOI		Saturation Level	<5 µm %	<10 µm %
			<100	>100	<100	>100			<100	>100			
VH-18	0.3	0.09	412	2	99.5	0.5	22.70	11	3.0	12.6	moist	21.80	39.00
VH-18	1.2	0.37	726	23	96.9	3.1	50.14	15	2.3	40.5	moist	10.40	17.70
VH-18	2.4	0.72	744	4	99.5	0.5	27.55	12	4.1	16.4	wet	20.80	37.70
VH-18	3.5	1.07	614	24	96.2	3.8	39.71	15	3.9	43.1	wet	17.20	30.70
VH-18	4.8	1.45	807	6	99.3	0.7	27.53	14	3.0	49.8	wet/pudding	20.40	36.50
VH-18	5.8	1.78	520	9	98.3	1.7	26.48	12	3.1	24.7	wet/pudding	22.10	39.40
VH-18	7.5	2.27	904	342	72.6	27.4	55.58	9	3.3	14.8	wet	11.50	20.30
VH-18	9.7	2.96	653	561	53.8	46.2	46.49	12	3.4	19.4	moist/wet	15.20	27.40
VH-18	11.6	3.54	1051	16	98.5	1.5	30.50	16	4.8	20.2	wet	20.10	36.00
VH-18	13.3	4.06	906	11	98.8	1.2	30.56	16	3.1	22.4	wet	19.20	34.10
VH-18	15.1	4.60	893	21	97.7	2.3	43.59	17	3.5	39.0	wet	13.20	23.70
VH-18	16.8	5.13	737	38	95.1	4.9	44.16	15	4.0	16.1	moist/wet	12.30	22.90
VH-18	17.9	5.45									loss		
VH-18	18.6	5.66	376	6	98.4	1.6	27.65	9	1.6	24.8	wet	20.10	36.00
VH-18	20.1	6.13	1154	11	99.1	0.9	20.52	15	2.6	8.1	wet	25.00	44.20
VH-18	21.7	6.62	564	3	99.5	0.5	18.18	12	2.3	8.1	wet	26.30	46.20
VH-18	23.6	7.19	1352	8	99.4	0.6	21.39	21	3.1	6.7	wet	23.50	41.90
VH-18	25.5	7.79	595	13	97.9	2.1	36.04	16	4.2	29.7	wet	17.10	30.70
VH-18	27.6	8.41	1513	19	98.8	1.2	18.83	29	2.7	5.8	wet	26.20	45.80
VH-18	29.9	9.12	1094	6	99.5	0.5	21.27	19	3.2	16.5	wet	25.10	44.50
VH-18	31.9	9.72	971	13	98.7	1.3	22.73	19	3.3	21.0	wet	22.20	41.10
VH-18	33.6	10.25	1018	13	98.7	1.3	28.94	20	3.2	12.9	wet	24.30	43.90
VH-18	35.1	10.69	616	132	82.4	17.6	56.71	14	3.7	29.0	wet	12.90	22.00

Hole #	Avg Depth (feet)	Avg Depth (meters)	Weight (g)		Weight %		Mean (μ m)	Gamma- Ray (cps)	% LOI		Saturation Level	<5 μ m %	<10 μ m %
			<100	>100	<100	>100			<100	>100			
VH-19	0.3	0.10	456	6	98.7	1.3	32.39	9	3.5	14.2	moist	18.00	34.30
VH-19	1.2	0.37	434	107	80.2	19.8	71.21	10	1.8	14.9	dry	6.67	12.10
VH-19	2.5	0.77	904	43	95.5	4.5	45.68	10	3.7	16.9	moist	15.10	27.00
VH-19	4.0	1.21	829	28	96.7	3.3	38.72	13	3.9	33.2	moist	15.70	28.20
VH-19	5.0	1.52	410	23	94.7	5.3	42.99	8	3.2	28.0	moist	15.50	27.10
VH-19	5.7	1.74	513	2	99.6	0.4	23.88	11	2.3	10.6	wet	22.60	39.70
VH-19	7.1	2.16	959	38	96.2	3.8	39.44	13	4.1	29.0	dry	16.50	29.60
VH-19	8.5	2.59	221	237	48.3	51.7	62.19	9	2.4	8.4	moist/dry	9.68	17.90
VH-19	9.5	2.91	190	257	42.5	57.5	67.26	5	5.2	38.6	dry	8.71	16.20
VH-19	10.6	3.23	285	123	69.9	30.1	62.84	9	2.7	21.2	dry	8.97	16.40
VH-19	12.2	3.71	760	158	82.8	17.2	67.68	8	4.4	33.2	moist/dry	6.97	12.80
VH-19	13.6	4.15	320	65	83.1	16.9	54.07	7	3.4	20.2	moist	10.70	19.80
VH-19	14.5	4.42	348	71	83.1	16.9	74.99	7	3.6	48.0	dry	6.40	11.30
VH-19	15.5	4.74	303	92	76.7	23.3	67.53	5	4.9	39.9	dry	8.40	15.30
VH-19	16.5	5.02	275	70	79.7	20.3	78.02	5	6.6	49.6	dry	5.96	10.80
VH-19	17.3	5.27	267	85	75.9	24.1	59.21	5	4.5	33.3	moist	9.66	17.90
VH-19	18.2	5.54	450	29	93.9	6.1	35.26	8	3.9	25.9	moist	17.50	32.10
VH-19	19.3	5.89	791	47	94.4	5.6	34.61	11	3.8	26.6	wet	17.60	32.10
VH-19	20.2	6.15	306	18	94.4	5.6	48.07	6	4.0	41.4	wet	10.90	20.50
VH-19	21.3	6.50	1042	21	98.0	2.0	42.07	11	4.0	24.7	wet	11.40	22.20
VH-19	23.2	7.07	825	24	97.2	2.8	31.48	11	9.9	10.8	wet	19.70	34.70
VH-19	24.7	7.54	790	25	96.9	3.1	22.35	18	2.1	5.2	wet	23.40	43.20
VH-19	26.0	7.92	532	7	98.7	1.3	22.43	8	2.8	14.8	wet	20.30	40.50
VH-19	27.8	8.48	1213	1	99.9	0.1	20.80	26	1.6	14.1	wet	17.90	35.40
VH-19	29.4	8.95	330	7	97.9	2.1	20.92	8	1.5	12.9	moist	21.10	40.60
VH-19	29.9	9.12	107	8	93.0	7.0	35.92	4	6.7	8.0	moist	10.10	22.70

Hole #	Avg Depth (feet)	Avg Depth (meters)	Weight (g)		Weight %		Mean (µm)	Gamma-Ray (cps)	% LOI		Saturation Level	<5 µm %	<10 µm %
			<100	>100	<100	>100			<100	<100			
VH-20	0.5	0.15	44	646	6.4	93.6	33.14	7	2.16	11.18	moist	17.8	32.3
VH-20	1.9	0.58	647	447	59.1	40.9	73.11	9	1.56	5.57	dry	10.0	18.5
VH-20	3.9	1.19	514	434	54.2	45.8	49.73	10	1.77	8.45	dry/moist	12.4	22.0
VH-20	5.5	1.68	329	273	54.7	45.3	54.49	11	2.60	3.48	moist	12.6	22.7
VH-20	7.0	2.13	1368	333	80.4	19.6	54.82	13	1.86	5.32	moist	14.2	25.8
VH-20	8.9	2.72	133	851	13.5	86.5	32.20	8	2.85	15.30	moist	14.1	26.8
VH-20	11.1	3.39	1656	133	92.6	7.4	66.82	7	3.55	8.48	moist	13.8	25.9
VH-20	13.2	4.01	70	608	10.3	89.7	72.19	7	3.13	8.87	moist	9.2	17.4
VH-20	15.0	4.56									loss		
VH-20	18.0	5.49	1002	162	86.1	13.9	88.78	7	3.22	8.11	moist	9.2	17.3
VH-20	20.7	6.31	898	447	66.8	33.2	60.15	7	3.71	8.75	pudding/moist	12.7	24.8
VH-20											liquid		